INTERNATIONAL CENTER FOR NUMERICAL METHODS IN ENGINEERING

Stabilization Techniques for Finite Element Analysis of Convection-Diffusion Problems

E. Oñate
M. Manzan

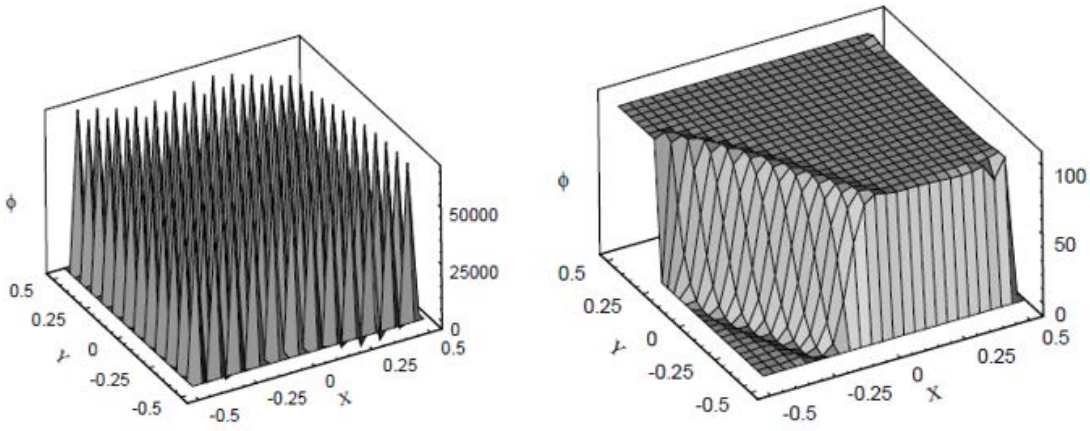

Publication CIMNE Nº-183, February 2000

Stabilization Techniques for Finite Element Analysis of Convection-Diffusion Problems

E. Oñate
M. Manzan

Publication CIMNE Nº-183, February 2000
Chapter of the book "Computational Analysis of Heat Transfer", G. Comini and B. Sundén (Eds.), WIT Press, Southampton, 2000

International Center for Numerical Methods in Engineering
Gran Capitán s/n, 08034 Barcelona, España

Stabilization techniques for finite element analysis of convection-diffusion problems

Eugenio Oñate[(1)] and Marco Manzan[(2)]
[(1)] *International Center for Numerical Methods in Engineering, Universidad Politécnica de Cataluña*
Gran Capitàn s/n, 08034 Barcelona, Spain
Email: onate@cimne.upc.es

[(2)] *Dipartimento di Energetica e Macchine,*
Università degli studi di Udine
via delle scienze 208, 33100 Udine, Italy
Email: marco@fthp1.dem.uniud.it

Abstract

The accurate solution of convection type problems on practical grids has been ever a challenging issue, and invariably some sort of stabilization is needed in order to get a physical solution. This has pushed researchers to develop various stabilization algorithms used in every day practice by numerical analysts. In this chapter some methods are presented along with a new finite increment calculus approach to obtain the different algorithms using higher order conservation equations.

1 Introduction

It is well known that the numerical methods used to solve convection type and fluid flow problems suffer from the inherently negative numerical diffusion when the centered type discretization is used for the advective terms.[1,2,4] This problem is shared by finite difference,[1,2] finite volume,[3] Galerkin finite element methods[4] and meshless procedures.[5–7] The lack of stability is shown by the presence of spurious node to node oscillations when the convective terms become important. These oscillations can be simply avoided by a smart refinement of the solution grid or mesh. Unfortunately this is not a viable solution due to the cost of simulations on very fine grids.

Several methods have been introduced in numerical literature to avoid this misbehavior. Among the more popular techniques we can name the so called Artificial Diffusion,[1,2,4] Streamline-Upwind Petrov-Galerkin (SUPG),[8,22] Generalized Galerkin,[23,24] Taylor-Galerkin,[4,25] Characteristic Galerkin (CG),[4,26] Galerkin Least Squares (GLS),[19,22,27,28] Subgrid Scale (SGS),[22,29–31] Bubble Functions[32–35] and Finite Increment Calculus (FIC)[36–40] procedures. In this chapter we will present some of these techniques used to obtain "stable" finite element solutions for the convection-diffusion equation.

Although the methods have been developed independently from each other, in this chapter we will show that the FIC method, based on a new concept of flow balance over a "finite size" domain, allows to reinterpret and derive most stabilized methods using physical arguments. Moreover, the FIC approach provides a general framework for computing the stabilization parameters in an objective manner. Examples of application of the FIC stabilization procedure to the solution of 1D and 2D convection-diffusion problems using the finite element method are presented.

2 The steady state convection-diffusion equation

Solution of the steady state convection-diffusion equation can be considered the starting point for the development of any numerical algorithm for solving more general transport equations such as those of convection-diffusion-reaction, viscous fluid flow, etc.

The steady state convection-diffusion equation can be written in general form as

$$-\mathbf{u}^T\boldsymbol{\nabla}\phi + \boldsymbol{\nabla}^T\mathbf{D}\boldsymbol{\nabla}\phi + Q = 0 \qquad \text{in} \quad \Omega \tag{1}$$

where ϕ is the transported variable (i.e. the temperature in a thermal problem or the concentration in a pollution transport problem, etc.), $\mathbf{u}$ is the velocity vector, $\boldsymbol{\nabla}$ is the gradient operator, $\mathbf{D}$ is the diffusivity matrix and Q is the source term. For 2D isotropic problems

$$\mathbf{u} = [u, v]^T, \quad \boldsymbol{\nabla} = \left\{ \begin{array}{c} \frac{\partial}{\partial x} \\ \frac{\partial}{\partial y} \end{array} \right\}, \quad \mathbf{D} = \begin{bmatrix} k & 0 \\ 0 & k \end{bmatrix} \tag{2}$$

where k is the diffusivity parameter.

The simplest boundary conditions associated to eqn. (1) are

$$\phi - \overline{\phi} = 0 \quad \text{on} \quad \Gamma_\phi \tag{3a}$$

$$\mathbf{n}^T\mathbf{D}\boldsymbol{\nabla}\phi + \overline{q}_n = 0 \quad \text{on} \quad \Gamma_q \tag{3b}$$

where Γ_ϕ and Γ_q denote the Dirichlet and Neumann parts of the analysis domain boundary Γ of $\Omega(\Gamma = \Gamma_\phi \cup \Gamma_q)$ where the variable and the normal flux are prescribed to values $\overline{\phi}$ and $\overline{q}_n$, respectively and $\mathbf{n}$ is the unit vector normal to the boundary Γ_q.

The transient form of eqn. (1) will be dealt with in Section 6.

2.1 Finite element discretization

Let us construct a finite element discretization over the analysis domain Ω. The standard interpolation within an element e with n nodes and area Ω^e can be written as[4]

$$\phi \simeq \hat{\phi} = \sum_{i=1}^{n} N_i \phi_i \tag{4}$$

where N_i are the element shape functions and ϕ_i are nodal values of the approximate function $\hat{\phi}$.

The discrete weighted residual form of eqns. (1)–(3) is written as

$$\int_\Omega w_i(-\mathbf{u}^T\boldsymbol{\nabla}\hat{\phi} + \boldsymbol{\nabla}^T\mathbf{D}\boldsymbol{\nabla}\hat{\phi} + Q)d\Omega + \int_{\Gamma_q} \overline{w}_i(\mathbf{n}^T\mathbf{D}\boldsymbol{\nabla}\phi + \overline{q}_n)d\Gamma = 0 \quad i = 1, N \tag{5}$$

In (5) w_i and $\overline{w}_i$ are test functions satisfying $w_i = \overline{w}_i = 0$ on Γ_ϕ and N is the total number of nodes in the mesh. Integration by parts of the diffusion term in the first integral of (5) and choosing $w_i = -\overline{w}_i$ gives

$$\int_\Omega (w_i\mathbf{u}^T\boldsymbol{\nabla}\hat{\phi} + (\boldsymbol{\nabla}^T w_i)\mathbf{D}\boldsymbol{\nabla}\hat{\phi})d\Omega = \int_\Omega w_i Q d\Omega - \int_{\Gamma_q} w_i\overline{q}_n d\Gamma - q_n^\phi \tag{6}$$

where q_n^ϕ is the outgoing normal flux across the Dirichlet boundary Γ_ϕ where the value of ϕ is prescribed. Note that q_n^ϕ can be computed "a posteriori" once the approximate solution $\hat{\phi}$ is found.

Eqn. (6) is usually written in matrix form

$$\mathbf{K}\hat{\boldsymbol{\phi}} = \mathbf{f} \tag{7}$$

where $\hat{\boldsymbol{\phi}} = [\phi_1, \phi_2 \cdots \phi_N]^T$ and matrix $\mathbf{K}$ and vector $\mathbf{f}$ are obtained by standard assembly of the element contributions given by

$$K_{ij}^{(e)} = \int_{\Omega^e} (w_i\mathbf{u}^T\boldsymbol{\nabla}N_j + \boldsymbol{\nabla}^T w_i\mathbf{D}\boldsymbol{\nabla}N_j)d\Omega \tag{8a}$$

$$f_i^{(e)} = \int_{\Omega^e} w_i Q d\Omega - \int_{\Gamma_q} w_i\overline{q}_n d\Gamma - q_n^\phi \tag{8b}$$

Indeed the terms involving $\overline{q}_n$ and q_n^ϕ in (8b) only appear when the element has a side over the boundaries Γ_q or Γ_ϕ, respectively.

The *Galerkin form* of eqns. (6) and (8) is simply obtained by making $w_i = N_i$. It is interesting to note that the equations resulting from the Galerkin FEM formulation using linear 1D elements coincide with those derived from the standard central finite difference scheme. Unfortunately, the discrete set of equations resulting from this choice is unstable, as shown next.

3 A simple example of the onset of numerical instability

Let us consider the simplest 1D convection-diffusion equation excluding the source term, i.e.

$$-u\frac{\mathrm{d}\phi}{\mathrm{d}x} + k\frac{\mathrm{d}^2\phi}{\mathrm{d}\,x^2} = 0 \tag{9}$$

Let us obtain the numerical solution of eqn. (9) in the 1D domain of Figure 1b of length $2l$ with the following Dirichlet boundary conditions

$$\begin{aligned} \phi &= 0 \quad at \quad x = 0 \\ \phi &= \bar{\phi} \quad at \quad x = 2l \end{aligned} \tag{10}$$

The "exact" analytical solution of eqn. (9) is:

$$\phi = A\, e^{\frac{u}{k}x} + B \tag{11}$$

where the constants A and B are computed from the boundary conditions at the two ends of the 1D domain.

For simplicity a numerical solution is attempted with the mesh of two equal size 2-node elements shown in Figure 1a. The application of the Galerkin finite element method (or the equivalent central finite difference scheme) leads in this case to the same system of equations as expected. This can be written as

$$-u\,\frac{\phi_3 - \phi_1}{2\,l} + k\,\frac{\phi_3 - 2\,\phi_2 + \phi_1}{l^2} = 0 \tag{12}$$

substitution of $\phi_1 = 0$ and $\phi_3 = \bar{\phi}$ from eqn. (10) gives

$$\phi_2 = \frac{1}{2}\,(1-\gamma)\,\bar{\phi} \tag{13}$$

where $\gamma = \frac{ul}{2k}$ is the so called element (or cell) Peclet number.

Note that for $\gamma = 0$ (i.e. the pure diffusive case) the solution $\phi_2 = \frac{\bar{\phi}}{2}$ coincides with the exact linear distribution shown in Figure 1b. However eqn. (13) shows clearly that ϕ_2 becomes negative for $\gamma > 1$. Indeed this is a non physical result as ϕ_2 should be $\geq 0\ \forall\ u, k$ as deduced from the exact solution (11) plotted in Figure 1b.

It is clearly deduced from this simple test that the standard numerical schemes (such as Galerkin FEM and central finite difference) fail for high values of the Peclet number (high u or small k). Indeed, the solution will improve with mesh refinement as a small value of the element length will also reduce the cell Peclet number so as to guarantee $\gamma > 1$. This however leads to prohibitive small element sizes for large values of the velocity.

3.1 Artificial diffusion scheme

A study of the truncation error of the Galerkin/Central difference scheme for the standard three nodes grid of Figure 2 leads to the following stencil

$$-u\,\frac{\phi_{i+1} - \phi_{i-1}}{2\,l} + k\,\frac{\phi_{i+1} - 2\,\phi_i + \phi_{i-1}}{l^2} = -u\phi_i' + (k - k^*)\,\phi_i'' \tag{14}$$

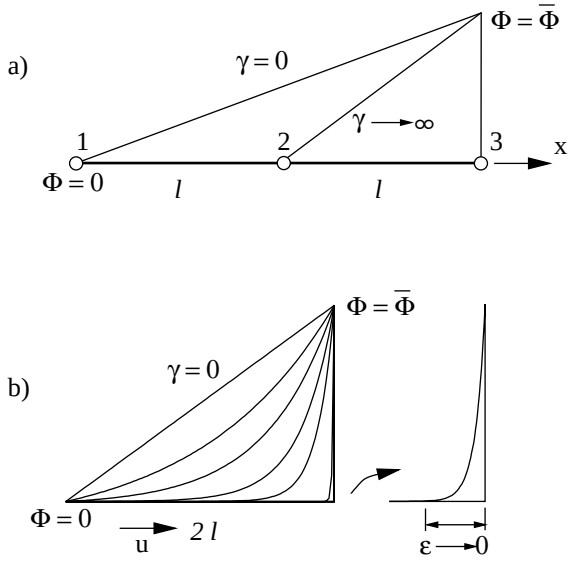

Figure 1: Simple 1d problem: a) two element discretization b) analytical solution

where $(\cdot)_i$ and $(\cdot)'$ denote values computed at point i and the x derivative respectively, and

$$k^* = \frac{k}{2\,\gamma}\left\{\sinh(2\,\gamma) - \frac{1}{\gamma}[\,\cosh(2\,\gamma) - 1]\right\} \geq 0 \tag{15}$$

is a positive constant which can be interpreted as an additional diffusion subtracting from the physical diffusion k. Eqn. (14) indicates that the numerical algorithm chosen solves in exact form at the nodes the following equation

$$-u\,\phi' + (k - k^*)\,\phi'' = 0 \tag{16}$$

A study of eqn. (15) shows that $k^* > k$ for $\gamma \geq 1$. Clearly for $k^* > k$ the "effective" diffusion in the numerical solution scheme becomes negative and this leads to the instability described in previous section.

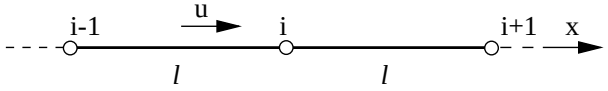

Figure 2: Simple 1d two element stencil

An obvious remedy to the "underdiffusive" character of the Galerkin/Central differences scheme is to add to the original differential equation an "artificial" or "balancing" diffusion term. From previous section it is clear that this diffusion term should be proportional to the Peclet number; i.e. it should increase with the velocity and the mesh size. The modified governing equation is therefore usually written as

$$-u\,\phi' + \left(k + \alpha\frac{u\,l}{2}\right)\,\phi'' = 0 \tag{17}$$

where $\alpha \geq 0$ is a parameter controlling the amount of "artificial diffusion" introduced into the balance differential equation.

Repetition of the simple two element example of Figure 1a starting now with eqn. (17) gives

$$\phi_2 = \frac{1}{(1+\alpha\,\gamma)}\;(1+\alpha\,\gamma-\gamma)\;\bar{\phi} \tag{18}$$

clearly $\phi_2 \geq 0$ if

$$\alpha \geq 1 - \frac{1}{\gamma} \tag{19}$$

which is the so called *critical value* of the stabilization parameter α ensuring a physical (stable) solution.

The value of α giving the "exact" solution at the nodes can be also simply obtained as follows. Eqn. (17) gives

$$\alpha = \frac{u\,\phi' - k\,\phi''}{\frac{u\,l}{2}\,\phi''} = \frac{2\,\phi'}{l\,\phi''} - \frac{1}{\gamma} \tag{20}$$

Application of the Galerkin/Central difference scheme yields

$$\begin{aligned} \alpha &= \frac{2\,\dfrac{\phi_{i+1}-\phi_{i-1}}{2\,l}}{l\,\dfrac{\phi_{i+1}-2\,\phi_i+\phi_{i-1}}{l^2}} - \frac{1}{\gamma} = \\ &= \frac{\phi_{i+1}-\phi_{i-1}}{\phi_{i+1}-2\,\phi_i+\phi_{i-1}} - \frac{1}{\gamma} \end{aligned} \tag{21}$$

Substitution of the exact solution (11) into (21) gives after small algebra

$$\alpha = \frac{e^{\gamma}+e^{-\gamma}}{e^{\gamma}-e^{-\gamma}} - \frac{1}{\gamma} = \coth\gamma - \frac{1}{\gamma} \tag{22}$$

which is the so called optimal value for the stability parameter α giving exact nodal solution values.[4,19]

The critical and optimal values of the stabilization parameter given by eqns. (19) and (22) practically coincide for $\gamma > 2$. The simplest expression (19) (which by the way does not require knowledge of the exact solution) is therefore chosen in practice.

3.2 Upwind finite difference scheme

Several authors soon blamed the central difference scheme (or the equivalent Galer-kin finite element method) as being the source of the numerical instabilities. An alternative difference scheme was proposed on the basis of a kind of "causality" argument: information downstream a point should not be used to provide insight on the changes in the convective term at the point. In other words, the convective derivative at a point should be computed using upstream information only. This was the conceptual origin of the "upwind" scheme which uses a backward difference to compute the convective derivative, while the diffusive term is still evaluated with the central difference formula.[1,2,41–43]

The upwind stencil for the two cell grid of Figure 2 may be therefore written as

$$-u\,\frac{\phi_i-\phi_{i-1}}{l}+k\,\frac{\phi_{i+1}-2\,\phi_i+\phi_{i-1}}{l^2}=0 \tag{23}$$

The solution of the simple Dirichlet problem of Figure 2 using above scheme is

$$\phi_2=\frac{1}{2\,(1+\gamma)}\,\bar{\phi} \tag{24}$$

note that $\phi_2 \to \bar{\phi}/2$ for $\gamma \to 0$ and $\phi_2 \to 0$ for $\gamma \to \infty$. Consequently, the upwind difference scheme preserves a physical solution as it eliminates the spurious negative values obtained with the full central difference scheme.

3.3 Relationship between the upwind difference scheme and the artificial diffusion method

Let us examine in detail the stencil obtained when applying the full central difference scheme (or the Galerkin FEM) to the modified equation (17) incorporating the artificial diffusion term. After very simple algebra we obtain

$$-u\,\frac{\phi_i-\phi_{i-1}}{l}\,\alpha-u\,\frac{\phi_{i+1}-\phi_{i-1}}{2\,l}\,(1-\alpha)+k\,\frac{\phi_{i+1}-2\,\phi_i+\phi_{i-1}}{l^2}=0 \tag{25}$$

Note now that for $\alpha = 0$ the form of the full central difference scheme when applied to all terms of the original unmodified convection equation (9) is obtained (see eqn. (12) for $2 = i$). Alternatively for $\alpha = 1$ the stencil obtained with the upwind scheme is found (see eqn. (23)).

It is therefore concluded that the upwind scheme provides the same stable solution that the artificial diffusion method for the limit value of $\alpha = 1$. This explains the well known fact that the upwind scheme yields generally over-diffusive results. Obviously, the exact nodal solution for all the range of Peclet numbers is no longer possible with the upwind scheme as this only yields accurate results for large values of the Peclet number.

Eqn. (25) also provides a very instructive interpretation of the artificial diffusion method. The parameter α can be viewed as an interpolation parameter providing values of the convective derivative term ranging from the expression of the central difference scheme ($\alpha = 0$) and that of the backward difference (upwind) scheme ($\alpha = 1$). Obviously the optimal value of α given by eqn. (22) must be used in order to obtain an exact nodal solution for any value of the Peclet number.

3.4 Petrov-Galerkin scheme

The deficiencies observed in the Galerkin FEM scheme led some authors to use a different class of weighting functions defined as[4, 8, 19, 44]

$$w_i = N_i + \alpha\, F_i \tag{26}$$

where N_i is the standard shape function of node i, F_i is a new test function and α is the stabilization parameter.

The resulting procedure is known as *Petrov-Galerkin* formulation as the weighting functions are now different from the shape functions.

It can be shown that for two node elements choosing $F_i = (-1)^{i+1}\ \frac{3}{4}\,(1-\xi^2)$ leads to the same stable stencil for the sourceless case given by eqn. (25).[16] This obviously also leads to the same optimal value for the stabilization parameter of eqn. (22).

A popular Petrov-Galerkin procedure is based on the following definition for the weighting function

$$w_i = N_i + \frac{\alpha\, l}{2}\frac{\mathrm{d}N_i}{\mathrm{d}x} \tag{27}$$

where l is the element length.

The weighted residual form for 1D Dirichlet problems is now written as

$$\int_L \left(N_i + \frac{\alpha\, l}{2}\frac{\mathrm{d}N_i}{\mathrm{d}x}\right)\left(-u\,\frac{\mathrm{d}\hat{\phi}}{\mathrm{d}x} + k\,\frac{\mathrm{d}^2\hat{\phi}}{\mathrm{d}\,x^2} + Q\right)\,dx = 0 \tag{28}$$

where L is the length of the 1D domain.

Note that the derivative $\frac{\mathrm{d}N_i}{\mathrm{d}x}$ is discontinuous between elements. This problem is overcome by applying the discontinuous weighting term on the element interiors only. Eqn. (28) is therefore usually written as

$$\begin{aligned}\int_L N_i \left(-u\,\frac{\mathrm{d}\hat{\phi}}{\mathrm{d}x} + k\,\frac{\mathrm{d}^2\hat{\phi}}{\mathrm{d}\,x^2} + Q\right)\,dx + \\ + \sum_{n_e}\int_{l^e}\frac{\alpha\, l^e}{2}\frac{\mathrm{d}N_i}{\mathrm{d}x}\left(-u\,\frac{\mathrm{d}\hat{\phi}}{\mathrm{d}x} + k\,\frac{\mathrm{d}^2\hat{\phi}}{\mathrm{d}\,x^2} + Q\right)\,dx = 0\end{aligned} \tag{29}$$

where the sum in the second term is taken over all the elements n_e and l^e is the length of element e.

Eqn. (29) is usually termed *consistent perturbed Galerkin form* as it adds to the original Galerkin expression a term which is residual based; that is, a term which vanishes as the numerical solution approaches the exact analytical value.[22]

A general expression of the perturbed Galerkin form can be written as

$$\int_L N_i\,\hat{r}\,dx - \sum_{n_e}\int_{l^e}\tau^e\,P(N_i)\,\hat{r}\,dx = 0 \tag{30}$$

where τ^e is the so called *intrinsic time parameter* defined for each element as

$$\tau^e = \frac{\alpha\, l^e}{2\,|u|} \tag{31}$$

and $P(\cdot)$ is a stabilizing operator acting on the shape functions N_i. Clearly in eqn. (29) $P := -u\,\frac{\mathrm{d}}{\mathrm{d}x}$. Obviously, many other forms for P are possible as shown later.

The term $\hat{r}$ in eqn. (30) denotes the point-wise error or "residual" of the numerical solution at each mesh point given by

$$\hat{r} = -u\,\frac{\mathrm{d}\hat{\phi}}{\mathrm{d}x} + k\,\frac{\mathrm{d}^2\hat{\phi}}{\mathrm{d}\,x^2} + Q \tag{32}$$

3.5 Equivalence of the Petrov-Galerkin scheme and the artificial diffusion scheme

Let us apply the standard Galerkin method to the modified equation (17) incorporating the artificial diffusion term; i.e.

$$\int_L N_i \left[-u \frac{\mathrm{d}\hat{\phi}}{\mathrm{d}x} + \left(k + \alpha \frac{u\, l}{2} \right) \frac{\mathrm{d}^2\hat{\phi}}{\mathrm{d}\, x^2} \right] dx = 0 \tag{33}$$

The term $\alpha \frac{u\, l}{2} \frac{\mathrm{d}^2\phi}{\mathrm{d}\, x^2}$ is now integrated by parts to give

$$\int_L \left[\left(N_i + \alpha \frac{l}{2} \frac{\mathrm{d}N_i}{\mathrm{d}x} \right) \left(-u \frac{\mathrm{d}\hat{\phi}}{\mathrm{d}x} \right) + N_i\, k \frac{\mathrm{d}^2\hat{\phi}}{\mathrm{d}\, x^2} \right] dx + b.c. = 0 \tag{34}$$

Eqn. (34) clearly shows that application of the Galerkin method to the artificial diffusion equation leads to a Petrov-Galerkin weighting of the convective term using the test functions w_i given by eqn. (27). Note also that in the case of linear elements and $Q = 0$ eqns. (28) and (34) are identical as the term $\frac{\alpha\, l}{2} \frac{\mathrm{d}N_i}{\mathrm{d}x}\, k \frac{\mathrm{d}^2\hat{\phi}}{\mathrm{d}\, x^2}$ in (28) vanishes (even after integration by parts!). This explains why the artificial diffusion scheme and the Petrov-Galerkin scheme with w_i defined as in eqn. (27) give the same result for the solution of eqn. (9).

This equivalence does not apply if the source term is taken into account. Hence although both the artificial diffusion method and the consistent Petrov-Galerkin formulation give stable results, the latter procedure is recommended for consistency and accuracy reasons.[4]

3.6 Galerkin Least Squares method

The Galerkin Least Square (GLS) method can be formulated as a particular case of the general Petrov-Galerkin procedure with the weighting functions defined as [19, 22, 27, 28]

$$w_i = N_i + \tau^e \left(-u \frac{\mathrm{d}N_i}{\mathrm{d}x} + k \frac{\mathrm{d}^2 N_i}{\mathrm{d}\, x^2} \right) \tag{35}$$

The GLS method can also be seen as a particular class of a perturbed Galerkin method written as

$$\begin{aligned} &\int_L N_i \left(-u \frac{\mathrm{d}\hat{\phi}}{\mathrm{d}x} + k \frac{\mathrm{d}^2\hat{\phi}}{\mathrm{d}\, x^2} + Q \right) dx - \\ &\quad - \sum_{n_e} \int_{l^e} \tau^e \left(-u \frac{dN_i}{dx} + k \frac{\mathrm{d}^2 N_i}{\mathrm{d}\, x^2} \right) \left(-u \frac{\mathrm{d}\hat{\phi}}{\mathrm{d}x} + k \frac{\mathrm{d}^2\hat{\phi}}{\mathrm{d}\, x^2} + Q \right) dx = 0 \end{aligned} \tag{36}$$

Comparison of eqns. (30) and (36) gives the form of the stabilization operator for the GLS method as

$$P := -u \frac{\mathrm{d}}{\mathrm{d}x} + k \frac{\mathrm{d}^2}{\mathrm{d}\, x^2} \tag{37}$$

The name least-squares in the GLS method emerges as the second term in eqn. (36) can be interpreted as the minimization of the following functional

$$\mathcal{I} = \sum_{n_e} \int_{l^e} \tau^e \left(-u \frac{\mathrm{d}\hat{\phi}}{\mathrm{d}x} + k \frac{\mathrm{d}^2\hat{\phi}}{\mathrm{d}\, x^2} + Q \right)^2 dx \tag{38}$$

which is a typical approach used in least-square approximation procedures.

3.7 The Subgrid Scale method

The Subgrid Scale (SGS) method, first introduced by Hughes,[29–31] has demonstrated to be a general method able to generate various different stabilized methods. A particular form of the SGS method was proposed by Douglas and Wang[45] for the Stokes problem, and then extended by Franca *et al.*[17] for the convection-diffusion equation. A generalization of the SGS method for incompressible flows has been recently proposed by Codina.[46] The SGS formulation is very similar to the GLS method, the only difference being the sign of the diffusive term in the operator $P(\cdot)$ of eqn. (37).

The basis of the SGS method is the assumption that the numerical solution of the governing differential equations is viewed as a multiscale phenomena where two sets of scales are present. Clearly, only the large scales can be resolved by the computational grid, whereas the small scales, defined as subgrid scales, are much smaller than the element or cell dimension.

We will present in this section the development of the method for the 1D steady state convection-diffusion equation (9) with Dirichlet boundary conditions (10).

The presence of two sets of scales suggests the splitting of the field variable, as $\phi = \hat{\phi} + \phi^*$ where $\hat{\phi}$, and ϕ^* represent the large and small scales respectively. As a consequence only $\hat{\phi}$ can be resolved by the mesh.

To proceed further the SGS method needs now a strong assumption: the unresolvable scales ϕ^* are forced to vanish on the element boundaries, i.e. $\phi^* = 0$ at $x = 0$ and $x = l^e$ for $e = 1, 2, \ldots, n_{\mathrm{e}}$.

The same splitting is applied to the test function, i.e. $w = \hat{w} + w^*$ where $\hat{w}$ and w^* are again the resolvable and unresolvable contributions respectively and $w^* = 0$ at the element boundaries.

Introducing the splitting of the variable and the test function into the weighted residual approximation of the 1D Dirichlet problem (viz eq.(5) with $\bar{w}_i = 0$) two sets of equation are obtained, one for the resolved scales

$$\int_L \left[\left(-u\frac{\mathrm{d}\hat{\phi}}{\mathrm{d}x} + k\frac{\mathrm{d}^2\hat{\phi}}{\mathrm{d}\,x^2} \right) \hat{w}_i + \left(-u\frac{\mathrm{d}\phi^*}{\mathrm{d}x} + k\frac{\mathrm{d}^2\phi^*}{\mathrm{d}\,x^2} \right) \hat{w}_i + Q\hat{w}_i \right] \, dx = 0 \tag{39}$$

and one for the unresolved scales

$$\int_L \left[\left(-u\frac{\mathrm{d}\hat{\phi}}{\mathrm{d}x} + k\frac{\mathrm{d}^2\hat{\phi}}{\mathrm{d}\,x^2} \right) w_i^* + \left(-u\frac{\mathrm{d}\phi^*}{\mathrm{d}x} + k\frac{\mathrm{d}^2\phi^*}{\mathrm{d}\,x^2} \right) w_i^* + Qw_i^* \right] \, dx = 0 \tag{40}$$

The Euler-Lagrange equations for eqn. (40) are

$$-u\frac{\mathrm{d}\phi^*}{\mathrm{d}x} + k\frac{\mathrm{d}^2\phi^*}{\mathrm{d}\,x^2} = -\hat{r} \tag{41}$$

$$\phi^* = 0 \quad for \quad x = 0, x = l^e \tag{42}$$

where the residual $\hat{r}$ is defined as in eqn. (32). Note that in eqn. (41) the unresolved part of the unknown ϕ^* is driven by the residual of the resolved part $\hat{\phi}$. Furthermore, due to the strong form of the Dirichlet boundary conditions, the problem is made local, that is it can be solved on the element interiors.

Problem (41) can be solved using a Green's function g giving

$$\phi^*(x) = \int_{l^e} g(x,y)\hat{r}(y)dy \tag{43}$$

where the Green's function $g(x,y)$ is the solution of the following equations

$$-u\frac{\mathrm{d}g}{\mathrm{d}x} + k\frac{\mathrm{d}^2 g}{\mathrm{d}\,x^2} = \delta(y-x) \tag{44a}$$

with

$$g = 0 \quad for \quad x = 0, x = l^e \tag{44b}$$

where $\delta(\cdot)$ is the Dirac delta function. As an example in Figure 3 the form of the Green's functions $g(x,y)$ for $y = 0.6$ and different values of the Peclet number are plotted.

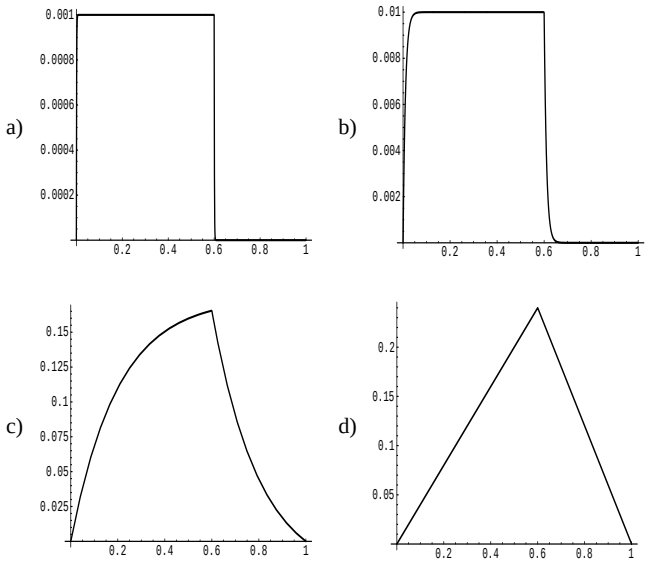

Figure 3: Element Green's function for the 1D advection-diffusion problem, a) $\gamma = 500$, b) $\gamma = 40$, c) $\gamma = 1$, d) $\gamma = 0$.

A stabilized numerical algorithm can be now obtained integrating by parts the second term of eqn. (39) giving

$$\begin{aligned}\int_L \left(-u\frac{\mathrm{d}\hat{\phi}}{\mathrm{d}x} + k\frac{\mathrm{d}^2\hat{\phi}}{\mathrm{d}\,x^2} + Q\right)\hat{w}_i dx \\ + \sum_{n_e}\int_{l^e}\left(u\frac{\mathrm{d}\hat{w}_i}{\mathrm{d}x}\phi^* - k\frac{\mathrm{d}\phi^*}{\mathrm{d}x}\frac{\mathrm{d}\hat{w}_i}{\mathrm{d}x}\right)dx = 0\end{aligned} \tag{45}$$

In eqn. (45) the boundary terms have canceled as w and w^* (and, consequently, $\hat{w} = w - w^*$) vanish on $x = 0$ and $x = L$.

As usual the second integral in eqn. (45) is computed on the element interiors only to account for the discontinuity of the derivatives of the weighting function $\hat{w}$ between elements.

Integrating by parts again the second term of the second integral of (45) gives

$$\int_L \left(-u\frac{\mathrm{d}\hat{\phi}}{\mathrm{d}x} + k\frac{\mathrm{d}^2\hat{\phi}}{\mathrm{d}\,x^2} + Q\right)\hat{w}dx + \sum_e \int_{l^e} \left(u\frac{\mathrm{d}\hat{w}}{\mathrm{d}x} + k\frac{\mathrm{d}^2\hat{w}}{\mathrm{d}\,x^2}\right)\phi^* dx = 0 \tag{46}$$

where again the boundary terms automatically vanish.

Substituting the value of ϕ^* from (43) into (46) gives finally

$$\int_L \hat{w}\hat{r}dx - \int_{l'_x}\int_{l'_y} \left(-u\frac{\mathrm{d}\hat{w}}{\mathrm{d}x} - k\frac{\mathrm{d}^2\hat{w}}{\mathrm{d}\,x^2}\right) g(x,y)\;\hat{r}(y)\;dy\;dx = 0 \tag{47}$$

where

$$\int_{l'} = \sum_{n_e} \int_{l^e} \tag{48}$$

and $\hat{r}$ is given by eqn. (32).

Eqn. (47) can be cast in the form of eqn. (30) if the Green's function $g(x,y)$ is approximated in a suitable way. For example the following assumption can be made

$$g(x,y) \approx \tilde{g}(x,y) := \tau(y)\cdot\delta(y-x) \tag{49}$$

where $\tau(y)$ is the stabilization function and δ is the Dirac delta function. Inserting eqn. (49) into (46) gives

$$\int_L \hat{w}\hat{r}dx - \sum_e \int_{l^e} \left(-u\frac{\mathrm{d}\hat{w}}{\mathrm{d}x} - k\frac{\mathrm{d}^2\hat{w}}{\mathrm{d}\,x^2}\right)\tau\;\hat{r}(x)\;dx = 0 \tag{50}$$

Note that in this case the operator $P(\cdot)$ of eqn. (30) is

$$P := -u\frac{\mathrm{d}}{\mathrm{d}x} - k\frac{\mathrm{d}^2}{\mathrm{d}\,x^2} \tag{51}$$

Comparison of eqns. (51) and (37) show that the differences between the SGS and GLS schemes arise only in the sign of the stabilizing diffusive term in P.

Eqn. (49) can be also used to obtain a formula for the computation of the stabilization function. A double integration gives

$$\int_{l^e}\int_{l^e} \tau\cdot\delta(y-x)dxdy = \int_{l^e}\int_{l^e} g(x,y)dxdy \tag{52}$$

For the simple 1D sourceless case and equal order elements the expression of τ is found as[29,31]

$$\tau = \frac{1}{l}\int_{l^e}\int_{l^e} g(x,y)\;dx\;dy = \frac{l}{2\,u}\;(\coth\gamma - \frac{1}{\gamma}) \tag{53}$$

Substituting eqn.(53) into (31) gives the expression of the optimal stabilization parameter $\alpha = \coth\gamma - \frac{1}{\gamma}$. The same expression was obtained in eqn. (22) using very different arguments.

4 Finite Increment Calculus procedure

The methods presented in the previous sections, although widely used in practice, are based on somewhat heuristic arguments. They require the addition of some balancing terms and the effectiveness of the underlying method is ruled by a quite mysterious stabilization parameter. In this section it will be shown how the stabilization terms appearing in the schemes so far described, emerge naturally applying higher order flow balance (or equilibrium) laws over a "finite" size domain.

4.1 Basic stabilized equation

Let us consider eqns. (9) to be solved in 1D domain of length L (Figure 4a). Figure 4b shows a typical segment AB of length $\overline{AB} = h$ where balance of fluxes must be satisfied.[36]

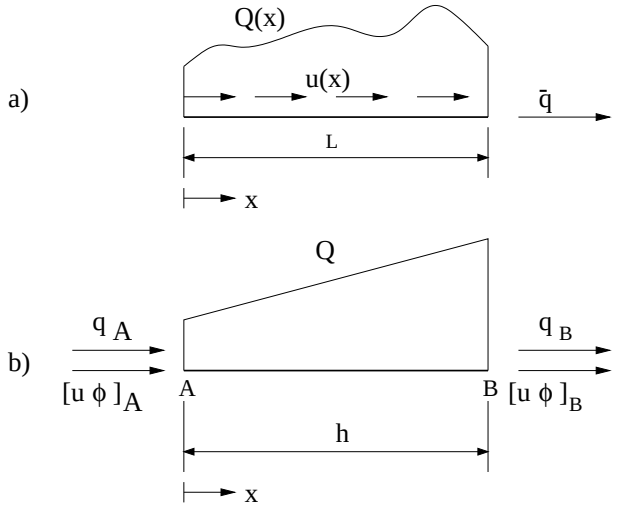

Figure 4: (a) One dimensional convection-diffusion problem. (b) Finite balance domain AB

Assuming a linear distribution of the external source Q over AB, the balance of fluxes between points A and B can be written as

$$q(x) + [u\phi](x) - q(x-h) - [u\phi](x-h) - \frac{1}{2}[Q(x) + Q(x-h)]\, h = 0 \tag{54}$$

The values of the diffusive flow rate q and the advective transport rate $u\phi$ at point A can be approximated starting with values at point B and using a higher order Taylor's expansion, i.e.

$$[u\phi](x_B - h) = [u\phi](x_B) - h\frac{\mathrm{d}[u\phi]}{\mathrm{d}x}\Big|_B + \frac{h^2}{2}\frac{\mathrm{d}^2[u\phi]}{\mathrm{d}\,x^2}\Big|_B - O(h^3) \tag{55}$$

$$q(x-h) = q(x) - h\frac{\mathrm{d}q}{\mathrm{d}x} + \frac{h^2}{2}\frac{\mathrm{d}^2 q}{\mathrm{d}\,x^2} - O(h^3) \tag{56}$$

$$Q(x-h) = Q(x) - h\frac{\mathrm{d}Q}{\mathrm{d}x} + O(h^2) \tag{57}$$

Substituting eqns. (55), (56) and (57) into (54) gives after simplification (taking u = constant)

$$-u\frac{\mathrm{d}\phi}{\mathrm{d}x}+\frac{\mathrm{d}}{\mathrm{d}x}\left(k\frac{\mathrm{d}\phi}{\mathrm{d}x}\right)+Q-\frac{h}{2}\frac{\mathrm{d}}{\mathrm{d}x}\left[-u\frac{\mathrm{d}\phi}{\mathrm{d}x}+\frac{\mathrm{d}}{\mathrm{d}x}\left(k\frac{\mathrm{d}\phi}{\mathrm{d}x}\right)+Q\right]=0 \tag{58}$$

Eqn. (58) can be rewritten in a more compact form as[36]

$$r-\frac{h}{2}\frac{\mathrm{d}r}{\mathrm{d}x}=0 \qquad , \qquad 0<x<L \tag{59}$$

where

$$r=-u\frac{\mathrm{d}\phi}{\mathrm{d}x}+k\frac{\mathrm{d}^2\phi}{\mathrm{d}\,x^2}+Q \tag{60}$$

Note that for $h=0$ the standard infinitesimal form of the 1D convection-diffusion equations (see eqn. (9)) is obtained.

4.1.1 Stabilized Neumann boundary condition

The essential (Dirichlet) boundary condition for eqn. (59) is the standard one given by eqn. (3a). For consistency a stabilized Neumann boundary condition must be obtained.

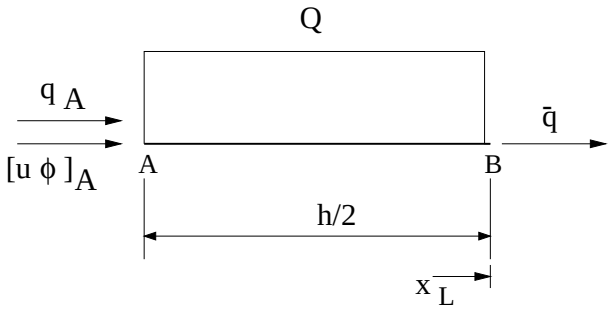

Figure 5: Balance domain next to a Neumann boundary point B

The length of the balance segment AB next to a Neumann boundary is taken now as one half of the characteristic length h for the interior domain (Figure 5). The balance equation, assuming a constant distribution for the source Q over AB, is now

$$\bar{q}-q(x_A)-[u\phi]_A-\frac{h}{2}Q=0 \tag{61}$$

where $\bar{q}$ is the prescribed total flux at $x=L$ and $x_A=x_B-\frac{h}{2}$.

Using a second order expansion for the advective and diffusive fluxes at point A gives[36]

$$-u\phi+k\frac{\mathrm{d}\phi}{\mathrm{d}x}+\bar{q}-\frac{h}{2}r \qquad on \quad x=L \tag{62}$$

where r is given by eqn. (60).

Note that if only the diffusive flux is prescribed at the Neumann boundary eqn. (62) modifies as

$$k\frac{\mathrm{d}\phi}{\mathrm{d}x}+\bar{q}-\frac{h}{2}r \qquad on \quad x=L \tag{63}$$

Again for $h=0$ the infinitesimal form of the 1D Neumann boundary conditions is obtained.

4.2 Equivalence with the artificial diffusion scheme

A particular case of the general stabilized equation can be obtained neglecting the diffusive and source parts in the term multiplied by h in eqn. (58) yielding

$$-u\frac{\mathrm{d}\phi}{\mathrm{d}x}+\frac{\mathrm{d}}{\mathrm{d}x}\left(k\frac{\mathrm{d}\phi}{\mathrm{d}x}\right)+Q+\frac{h}{2}\frac{\mathrm{d}}{\mathrm{d}x}\left(u\frac{\mathrm{d}\phi}{\mathrm{d}x}\right)=0 \tag{64}$$

Writing the characteristic length h as $h=\alpha l$, where l is the element or cell size, gives

$$-u\frac{\mathrm{d}\phi}{\mathrm{d}x}+\frac{\mathrm{d}}{\mathrm{d}x}\left(k+\alpha\frac{ul}{2}\right)\frac{\mathrm{d}\phi}{\mathrm{d}x}+Q=0 \tag{65}$$

The analogy of eqn. (65) with the artificial diffusion method (see eqn. (17)) is readily seen.

4.3 Equivalence of the FIC method with the Petrov-Galerkin FE formulation

The standard Galerkin form for the FE solution of eqns. (59) and (63) is equivalent to the Petrov-Galerkin formulation described in Section 3.4.[36] To proof this let us construct a finite element discretization. Inserting eqn. (4) into (59) and (63) gives

$$\hat{r}-\frac{h}{2}\frac{\mathrm{d}\hat{r}}{\mathrm{d}x}=r_\Omega \qquad in \qquad 0\leq x\leq L \tag{66}$$

$$\hat{\phi}-\bar{\phi}=r_\phi \qquad \text{on} \qquad x=0 \tag{67a}$$

$$k\frac{\mathrm{d}\hat{\phi}}{\mathrm{d}x}+\bar{q}-\frac{h}{2}\hat{r}=r_q \qquad \text{on} \qquad x=L \tag{67b}$$

where $\hat{r}=r(\hat{\phi})$ and r_Ω, r_ϕ and r_q are the residuals of the approximate solution in the domain and on the Dirichlet and Neumann boundaries, respectively.

The weighted residual expression of eqns. (66) and (67) is

$$\int_0^L w_i\left(\hat{r}-\frac{h}{2}\frac{\mathrm{d}\hat{r}}{\mathrm{d}x}\right)dx+\left[\overline{w}_i\left(k\frac{\mathrm{d}\hat{\phi}}{\mathrm{d}x}+\bar{q}-\frac{h}{2}\hat{r}\right)\right]_{x=L}=0 \tag{68}$$

where as usual the test functions w_i and $\overline{w}_i$ are assumed to be zero on the Dirichlet boundary, therefore implying the satisfaction of the essential boundary conditions.[4]

Integrating by parts the term $w_i\frac{h}{2}\frac{\mathrm{d}\hat{r}}{\mathrm{d}x}$ in eqn. (68) in a distributional sense and choosing $\overline{w}_i=-w_i$ gives

$$\int_0^L w_i\hat{r}dx-\left[w_i\left(k\frac{\mathrm{d}\hat{\phi}}{\mathrm{d}x}+\overline{q}\right)\right]_{x=L}+\sum_{n_e}\int_{l^e}\frac{h}{2}\frac{\mathrm{d}w_i}{\mathrm{d}x}\hat{r}dx=0 \tag{69}$$

The Galerkin form is readily obtained by making $w_i=N_i$ in eqn. (69). Note the analogy of the resulting expression with the perturbed Galerkin form of eqn. (30) with $P=-\frac{h}{2}\frac{\mathrm{d}}{\mathrm{d}x}$. Also choosing $h=\alpha l^e$ eqn. (69) coincides with the form resulting from the Petrov-Galerkin scheme of eqn. (29).

4.3.1 *Equivalence of the FIC method with the Subgrid Scale model*

A stabilization scheme similar to the Subgrid Scale model can be obtained from the FIC method. Assuming a quadratic distribution of the source term Q, eqn. (54) can be rewritten as

$$q(x)+[u\phi](x)-q(x-h)-[u\phi](x-h)+\frac{h}{6}\left[Q(x)+4Q\left(x-\frac{h}{2}\right)+Q(x-h)\right]=0 \quad (70)$$

A new balance equation can be obtained by inserting in eqn. (70) Taylor's expansions up to third order of the advective and diffusive fluxes at point $(x-h)$ and up to second order for the source term at $(x-\frac{h}{2})$ and $(x-h)$.[37] This gives

$$r-\frac{h}{2}\frac{\mathrm{d}r}{\mathrm{d}x}+\frac{h^2}{6}\frac{\mathrm{d}^2 r}{\mathrm{d}\,x^2}=0 \quad (71)$$

where r is defined in eqn. (60).

The weighted residual form of eqn. (71) for the Dirichlet problem can be written as

$$\int_0^l w\left[\hat{r}-\frac{h}{2}\frac{\mathrm{d}\hat{r}}{\mathrm{d}x}+\frac{h^2}{6}\frac{\mathrm{d}^2\hat{r}}{\mathrm{d}\,x^2}\right]dx=0 \quad (72)$$

Integrating by parts once the term $w\frac{h}{2}\frac{\mathrm{d}\hat{r}}{\mathrm{d}x}$, twice the term $w\frac{h^2}{6}\frac{\mathrm{d}^2\hat{r}}{\mathrm{d}\,x^2}$ and making $w_i=N_i$ gives

$$\int_0^l N_i\hat{r}dx-\sum_e\int_{l^e}\left(-\frac{h}{2}\frac{\mathrm{d}N_i}{\mathrm{d}x}-\frac{h^2}{6}\frac{\mathrm{d}^2 N_i}{\mathrm{d}\,x^2}\right)\hat{r}dx+b.c.=0 \quad (73)$$

Note the analogy of this expression with eqn. (50) derived using the Subgrid Scale approach.

5 Multidimensional case

The Galerkin solution of the multidimensional equations (1)–(3) leads to the same unstability problems encountered when solving the 1D equation. The different stabilization techniques explained for the 1D case have been extended with different success to solve 2D and 3D problems. A summary of the basic ingredients of these extensions is given next.

5.1 Multidimensional artificial diffusion and perturbed Galer-kin forms

Extensions of the *artificial diffusion* scheme have followed the idea of adding the necessary balancing diffusion along the streamlines directions only. The modified differential equation in this case is

$$-\mathbf{u}^T\boldsymbol{\nabla}\phi+\boldsymbol{\nabla}^T(\mathbf{D}+\mathbf{D}^*)\boldsymbol{\nabla}\phi+Q=0 \quad (74)$$

where $\mathbf{D}^*=\frac{\alpha l^e}{2|\mathbf{u}|}\mathbf{u}\,\mathbf{u}^T$ is the additional diffusivity matrix, α is the stabilization parameter and l^e is a characteristic element dimension. Typically $l^e=(\Omega^e)^{1/d}$ with $d=1,2,3$ for 1D, 2D and 3D problems, respectively.

Let us write the Galerkin finite element form for the modified eqn. (74) (assuming Dirichlet boundary conditions). This gives

$$\int_\Omega N_i[-\mathbf{u}^T\boldsymbol{\nabla}\hat{\phi} + \boldsymbol{\nabla}^T(\mathbf{D}+\mathbf{D}^*)\boldsymbol{\nabla}\hat{\phi} + Q] = 0 \tag{75}$$

Integration by parts of the artificial diffusion term gives

$$\int_\Omega \left[-\left(N_i + \frac{\alpha l^e}{2|\mathbf{u}|}\mathbf{u}^T\boldsymbol{\nabla}N_i \right)\mathbf{u}^T\boldsymbol{\nabla}\hat{\phi} + N_i(\boldsymbol{\nabla}^T\mathbf{D}\boldsymbol{\nabla}\hat{\phi} + Q) \right] d\Omega + b.c. = 0 \tag{76}$$

Eqn. (76) clearly shows that introducing the artificial diffusion $\mathbf{D}^*$ leads to a Petrov-Galerkin weighting of the convective term similarly as in the 1D case (see eqn. (34)).

Above procedure has been widely used in practice choosing for α the optimal value deduced from the simplified 1D case (i.e. eq.(22) with $\gamma = \frac{|\mathbf{u}|l^{(e)}}{2k}$).[4, 10, 19, 39]

A more rigorous approach is based on the perturbed Galerkin form, i.e. viz eqn. (30) with $\hat{r} = -\mathbf{u}^T\boldsymbol{\nabla}\hat{\phi} + \boldsymbol{\nabla}^T\mathbf{D}\boldsymbol{\nabla}\hat{\phi} + Q$ and the following expressions for the perturbation function P

Method	**Perturbation function**	
Streamline Upwind Petrov-Galerkin (SUPG)	$P := -\mathbf{u}^T\boldsymbol{\nabla}$	(77a)
Galerkin Least-Square (GLS)	$P := -\mathbf{u}^T\boldsymbol{\nabla} + \boldsymbol{\nabla}^T\mathbf{D}\boldsymbol{\nabla}$	(77b)
Subgrid Scale (SGS)	$P := -\mathbf{u}^T\boldsymbol{\nabla} - \boldsymbol{\nabla}^T\mathbf{D}\boldsymbol{\nabla}$	(77c)

Note that the SUPG method adds a balancing diffusion along the streamline direction. The resulting integral expression is similar to eqn. (76), the difference being that the perturbation function is also affecting the diffusive and source terms in the SUPG case.

5.2 Multidimensional finite increment calculus formulation

Extending the concept of finite increment calculus (FIC) to 2D and 3D problems leads to the consistently modified differential equations[37]

$$r - \frac{1}{2}\mathbf{h}^T\boldsymbol{\nabla}r = 0 \quad \text{in} \quad \Omega \tag{78a}$$

$$\phi - \overline{\phi} = 0 \quad \text{on} \quad \Gamma_p \tag{78b}$$

$$\mathbf{n}^T\mathbf{D}\boldsymbol{\nabla}\phi + \overline{q}_n - \frac{1}{2}\mathbf{h}^T\mathbf{n}r = 0 \quad \text{on} \quad \Gamma_q \tag{78c}$$

with the characteristic vector $\mathbf{h}$ defined as (for 2D problems)

$$\mathbf{h} = [h_x, h_y]^T \tag{79}$$

Again note that for $\mathbf{h} = 0$ the infinitesimal form of the multidimensional convection-diffusion equations is obtained (see eqns. (1)–(3)).

Application of the Galerkin finite element method to eqns. (79) leads to the following integral expression (after integration by parts of the terms involving **h**)

$$\int_\Omega N_i \hat{r} d\Omega - \int_{\Gamma_q} N_i (\mathbf{n}^T \mathbf{D} \boldsymbol{\nabla} \phi + \overline{q}_n) d\Gamma + \sum_{n_e} \int_{\Omega^e} \frac{1}{2} \mathbf{h}^T \boldsymbol{\nabla} N_i \hat{r} d\Omega = 0 \tag{80}$$

The expression of the perturbation function P can be identified in this case as $P = -\frac{1}{2}\mathbf{h}^T \boldsymbol{\nabla}$.

A particular expression of **h** can be found if the characteristic vector is chosen aligned with the velocity vector, i.e. $\mathbf{h} = \frac{h}{|\mathbf{u}|}\mathbf{u}$, where h is a characteristic distance. Choosing $h = \alpha l^e$ where l^e is an element dimension recovers the form of the perturbation function defined for the SUPG method.[37] The *intrinsic time parameter* is now defined as

$$\tau = \frac{h}{2|\mathbf{u}|} \tag{81}$$

Note that this coincides with the time taken for a particle to travel the distance $h/2$ at the speed $|\mathbf{u}|$.

5.2.1 The role of the stabilizing crosswind dissipation

The assumption of the characteristic length vector **h** being parallel to the velocity vector **u** is a *simplification* which eliminates any transverse diffusion effect. However it is well known that when arbitrary sharp transverse layers are present, additional transverse (or crosswind) diffusion is required to capture these discontinuities. Different "ad hoc" expressions for the transverse diffusion terms, typically of non linear nature, have been proposed.[19,47–49] The introduction of this additional stabilizing effect can be simply reproduced in the FIC approach by abandoning the assumption of **h** being parallel to **u** and keeping the two characteristic lengths h_x and h_y as "free" stabilization parameters. A technique for computation of these two parameters is described in the following section.

5.2.2 Computation of the stabilization parameters in the FIC method

Let us consider the finite element solution of an advective-diffusive problem. The solution residual of the modified equation is

$$\hat{r} - \frac{1}{2}\mathbf{h}^T \boldsymbol{\nabla} \hat{r} = r_\Omega \qquad \text{in} \quad \Omega \tag{82}$$

where $\hat{r} = r(\hat{\phi})$ and $\hat{\phi}$ is the approximate finite element solution.

Let us now define the average residual of a particular numerical solution over an element as

$$r^{(e)} = \frac{1}{\Omega^{(e)}} \int_{\Omega^{(e)}} r_\Omega \, d\Omega \tag{83}$$

Substituting eqn. (82) into (83) gives

$$r^{(e)} = \hat{r}^{(e)} - \left(\frac{1}{2}\mathbf{h}^T \boldsymbol{\nabla} \hat{r} \right)^{(e)} \tag{84}$$

where

$$a^{(e)} := \frac{1}{\Omega^{(e)}} \int_{\Omega^{(e)}} a \, d\Omega \tag{85}$$

For simplicity the characteristic length vector will be assumed to be constant over each element, i.e. $\mathbf{h} = \mathbf{h}^{(e)}$. With this assumption eqn. (84) can be simplified to

$$r^{(e)} = \hat{r}^{(e)} - \frac{1}{2} \left[\mathbf{h}^{(e)}\right]^T (\boldsymbol{\nabla} \hat{r})^{(e)} \tag{86}$$

Let us express the characteristic length vector in terms of the components along the velocity vector $\mathbf{u}$ and an arbitrary direction $\mathbf{v}$ as

$$\mathbf{h} = h_s \frac{\mathbf{u}}{|\mathbf{u}|} + h_t \frac{\mathbf{v}}{|\mathbf{v}|} \tag{87}$$

where h_s and h_t are streamline and transverse (crosswind) characteristic lengths, respectively.

Excellent results have been found taking $\mathbf{v} = \boldsymbol{\nabla} \phi$ following the ideas of shock capturing schemes.[19,47–49] Other expressions for $\mathbf{v}$ are however possible and they should all lead to stable results.

Substituting eqn. (87) into (86) gives

$$r^{(e)} = \hat{r}^{(e)} - \frac{1}{2} \left[h_s \frac{\mathbf{u}^T}{|\mathbf{u}|} + h_t \frac{\mathbf{v}^T}{|\mathbf{v}|} \right]^{(e)} (\boldsymbol{\nabla} \hat{r})^{(e)} \tag{88}$$

The characteristic lengths h_s and h_t can be expressed now as a proportion of a typical element dimension $l^{(e)}$

$$h_s^{(e)} = \alpha_s^{(e)} l^{(e)} \quad , \quad h_t = \alpha_t^{(e)} l^{(e)} \tag{89}$$

where $\alpha_s^{(e)}$ and $\alpha_t^{(e)}$ are the streamline and transverse stabilization parameters, respectively. In the examples shown next $l^{(e)}$ has been taken equal to $(\Omega^e)^{1/d}$.

Clearly for $\alpha_t^{(e)} = 0$ just the streamline diffusion effect, typical of the SUPG approach, is reproduced.

Let us consider now that an enhanced numerical solution has been found for a given finite element mesh. This can be simply achieved by projecting into the original mesh an improved solution obtained via global/local smoothing or superconvergent recovery of derivatives.[4,50,51] If $r_1^{(e)}$ and $r_2^{(e)}$ respectively denote the element residuals of the original and the enhanced numerical solutions for a given mesh it is obvious that

$$r_1^{(e)} - r_2^{(e)} \geq 0 \tag{90}$$

Clearly in the limit case of the exact solution $r_1^{(e)} = r_2^{(e)} = 0$.

Eqn. (90) assumes that r_1 is positive. For the negative case the inequality should be appropriately reversed.

Combining eqns. (88), (89, (90) gives

$$[\alpha_s \frac{\mathbf{u}^T}{|\mathbf{u}|} + \alpha_t \frac{\mathbf{v}^T}{|\mathbf{v}|}]^{(e)} (\boldsymbol{\nabla} \hat{r}_2^{(e)} - \boldsymbol{\nabla} \hat{r}_1^{(e)}) \geq \frac{2}{l^{(e)}} (\hat{r}_2^{(e)} - \hat{r}_1^{(e)}) \tag{91}$$

Eqn (91) is the basis for computing iteratively the stabilization parameters α_s and α_t as shown in next section.

In the 2D examples of Section 5.4 solved with linear four node quadrilaterals the first derivatives of ϕ are first computed at the 2×2 Gauss points within each element. The enhanced derivative field is then computed by projecting the Gauss point values to the element nodes using a bi-linear interpolation and then averaging the discontinuous nodal values contributed by the elements sharing the node.

5.2.3 Alpha-adaptive stabilization scheme

The following scheme can be devised to obtain a stable numerical solution in an adaptive manner.[37,38]

1. Solve the stabilized problem defined by eqn. (78) using the FEM with an initial guess of the stabilization parameters, i.e.

$$\alpha_s^{(e)} = {}^o\alpha_s^{(e)} \quad , \quad \alpha_t^{(e)} = {}^o\alpha_t^{(e)} \tag{92}$$

2. Recover an enhanced derivatives field. Evaluate $\hat{r}_1^{(e)}, \hat{r}_2^{(e)}, \boldsymbol{\nabla}\hat{r}_1^{(e)}$ and $\boldsymbol{\nabla}\hat{r}_2^{(e)}$.

3. Compute an enhanced value of the streamline stabilization parameter $\alpha_s^{(e)}$ from eqn. (91) by

$${}^1\alpha_s^{(e)} = \frac{|\mathbf{u}|}{\mathbf{u}^T(\boldsymbol{\nabla}\hat{r}_2^{(e)} - \boldsymbol{\nabla}\hat{r}_1^{(e)})} \left[\frac{2}{l^{(e)}}(\hat{r}_2^{(e)} - \hat{r}_1^{(e)}) - \alpha_t^{(e)} \frac{\mathbf{v}^T}{|\mathbf{v}|}(\boldsymbol{\nabla}\hat{r}_2^{(e)} - \boldsymbol{\nabla}\hat{r}_1^{(e)}) \right] \tag{93}$$

4. Repeat steps (1)–(3) until convergence is found for the value of $\alpha_s^{(e)}$ while keeping $\alpha_t^{(e)}$ constant.

5. Repeat steps (1)–(4) for computing $\alpha_t^{(e)}$ while keeping $\alpha_s^{(e)}$ constant and equal to the previously converged value. In the first iteration $\alpha_t = {}^o\alpha^{(e)} + \varepsilon$, where ε is a small value, should be used. The updated value of $\alpha_t^{(e)}$ is computed as

$${}^i\alpha_t^{(e)} = \frac{|\mathbf{v}|}{\mathbf{v}^T(\boldsymbol{\nabla}\hat{r}_2^{(e)} - \boldsymbol{\nabla}\hat{r}_1^{(e)})} \left[\frac{2}{l^{(e)}}(\hat{r}_2^{(e)} - \hat{r}_1^{(e)}) - \alpha_s^{(e)} \frac{\mathbf{u}^T}{|\mathbf{u}|}(\boldsymbol{\nabla}\hat{r}_2^{(e)} - \boldsymbol{\nabla}\hat{r}_1^{(e)}) \right] \tag{94}$$

6. Once $\alpha_t^{(e)}$ has been found steps (1)–(5) can be repeated to obtain yet more improved values of both $\alpha_s^{(e)}$ and $\alpha_t^{(e)}$.

Details of the treatment of elements next to boundary can be found in Oñate *et al*.[38]

Note that for $\alpha_t^{(e)} = 0$ above adaptive scheme provides the value of the critical streamline stabilization parameter $\alpha_s^{(e)}$ corresponding to the SUPG procedure. Accounting for the cross-wind stabilization parameter α_t is essential for obtaining a stable solution in presence of arbitrary transverse sharp layers.

The number of iterations in the above adaptive process is substantially reduced if the initial guess for $\alpha_s^{(e)}$ and $\alpha_t^{(e)}$ are not far from the final converged values. This can be ensured by using as initial value for $\alpha_s^{(e)}$ the standard expression derived from the straight forward extension of the simple 1D case, whereas the initial guess ${}^o\alpha_t^{(e)} = 0$ provides a good approximation in zones far from sharp layers non orthogonal to the velocity vector.

5.3 Example: 1D convection-diffusion problem solved with FIC method

Particularizing eqn. (93) for the 1D convection-diffusion problem gives (making $\alpha_t^{(e)} = 0$)

$$\alpha^{(e)} \geq 2/l^{(e)} \left(\hat{r}_2^{(e)} - \hat{r}_1^{(e)}\right) \left[\left(\frac{d\hat{r}_2}{dx}\right)^{(e)} - \left(\frac{d\hat{r}_1}{dx}\right)^{(e)}\right]^{-1} \tag{95}$$

The equality case in eqn (95) yields the critical value of the element stabilization parameter ensuring no growth of the numerical error. The accuracy of above expression is shown next in a simple example.

Let us consider the FE solution of the sourceless 1D convection-diffusion problem

$$-u\frac{d\phi}{dx} + k\frac{d^2\phi}{dx^2} = 0, \qquad 0 \leq x \leq l \tag{96}$$

with boundary conditions

$$\begin{aligned} \phi &= 0 \quad \text{at} \quad x = 0 \\ \phi &= 1 \quad \text{at} \quad x = l \end{aligned} \tag{97}$$

The solution will be attempted with the simplest two node linear element. For a uniform mesh the residual and the average residual derivative over an element with nodes i and $i+1$ can be found as

$$\hat{r}_1^{(e)} = -\frac{u}{l^{(e)}}(\phi_{i+1} - \phi_i) \quad \text{and} \quad \left(\frac{d\hat{r}_1}{dx}\right)^{(e)} = 0 \tag{98}$$

The enhanced solution is obtained now by a simple smoothing of the first order convective derivative at the nodes. The elemental residual for the enhanced solution is given by

$$\hat{r}_2^{(e)} = -\frac{u}{2}(\hat{\phi}'_i + \hat{\phi}'_{i+1}) + \frac{k}{l^{(e)}}(\hat{\phi}'_{i+1} - \hat{\phi}'_i) \tag{99}$$

where $\hat{\phi}'_i = \left(\frac{d\hat{\phi}}{dx}\right)_i$. A simple algebra gives

$$\hat{r}_2^{(e)} = -\frac{u}{4l^{(e)}}(\phi_{i+1} - \phi_{i-1} + \phi_{i+2} - \phi_i) + \frac{k}{2(l^{(e)})^2}(\phi_{i+2} - \phi_i - \phi_{i+1} + \phi_{i-1}) \tag{100}$$

A similar procedure leads to (neglecting the third order derivative term)

$$\left(\frac{d\hat{r}_2}{dx}\right)^{(e)} = -u\frac{d^2\hat{\phi}}{dx^2} = -\frac{u}{2(l^{(e)})^2}[\phi_{i+2} - \phi_i - \phi_{i+1} + \phi_{i-1}] \tag{101}$$

Substituting above equations into (95) gives the element critical stabilization parameter

$$\alpha^{(e)} \geq \left[\frac{\phi_{i+2} - 3\phi_{i+1} + 3\phi_i - \phi_{i-1}}{\phi_{i+2} - \phi_{i+1} - \phi_i + \phi_{i-1}} - \frac{1}{\gamma}\right] \tag{102}$$

where $\gamma = \frac{ul^{(e)}}{2k}$ is the element Peclet number.

It can be checked that the value of $\alpha^{(e)}$ given by eqn. (102) coincides in this case with the analytical expression typically used in practice. For this purpose let us substitute into eqn. (102) the general numerical solution for this problem given by

$$\phi_i = A + B\left[\frac{1+\gamma(\alpha+1)}{1+\gamma(\alpha-1)}\right]^i \tag{103}$$

where A and B are constants. After same simple algebra we obtain[37]

$$\alpha^{(e)} \geq 1 - \frac{1}{\gamma} \tag{104}$$

which coincides with the standard critical value (see eqn. (19)).

Figures 6 and 7 show practical applications of the iterative (adaptive) process for computing α explained in Section 5.2.3. In the first case the solution of the 1D convection-diffusion problem is attempted for $\gamma = 5$ using a mesh of twenty linear elements. An initial value of ${}^0\alpha^{(e)} = 0.5$ is chosen for all elements. Figure 6 (a) shows the convergence of the solution for $\alpha^{(e)}$. Note that the critical value $\alpha^{(e)} = 0.8$ is obtained in all elements after a few iterations. Figure 6 (b) also displays the convergence of the numerical solution for ϕ showing convergence to the "exact" solution after three iterations.

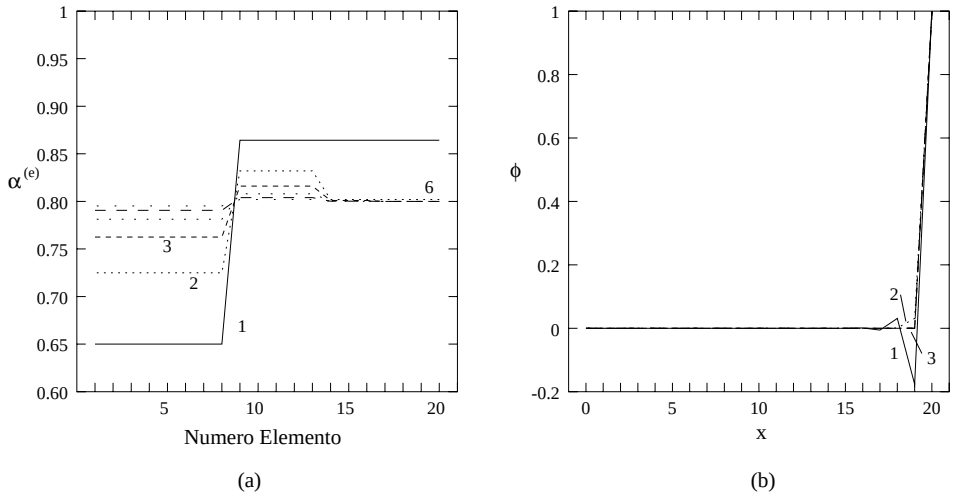

Figure 6: One dimensional advection-diffusion problem. Convergence of the critical value of the element stabilization parameter $\alpha^{(e)}$ (a) and of the numerical solution ϕ (b) obtained with 20 two node linear elements. Peclet number $\gamma = 5$

Results for the same problem for $\gamma = 25$ are shown in Figure 7. Note that as in previous example a good solution is obtained with just two iterations. Seven iterations are however needed to obtain the critical value of $\alpha^{(e)}$ for all elements. Indeed in both cases it suffices to obtain a good approximation for $\alpha^{(e)}$ in the vicinity of the right hand node and this always occurs after 2-3 iterations.

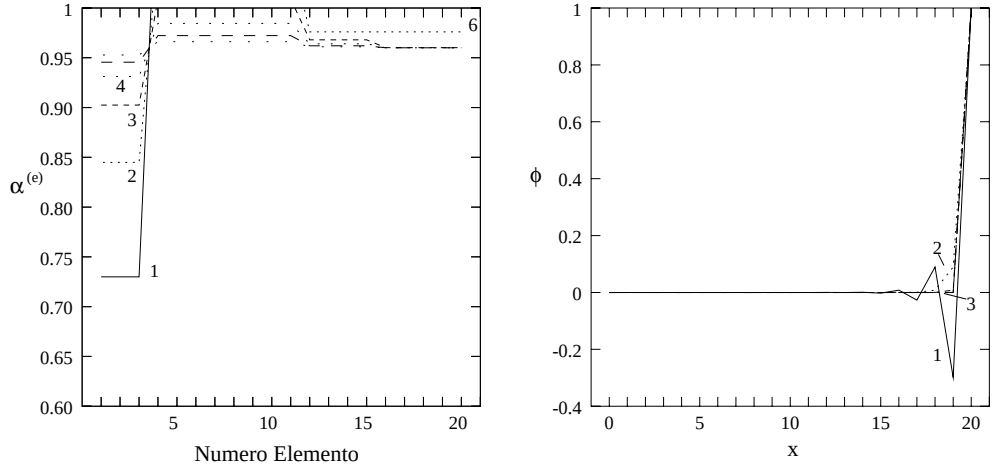

Figure 7: One dimensional advection-diffusion problem. Convergence of the critical value of the element stabilization parameter $\alpha^{(e)}$ (a) and of the numerical solution ϕ (b) obtained with 20 two node linear elements. Peclet number $\gamma = 25$

5.4 2D convection problems solved with FIC method

5.4.1 Two dimensional advective-diffusive problem with no source, diagonal velocity and uniform Dirichlet boundary conditions

The first 2D example chosen is the solution of the standard advection-diffusion equation in a square domain of unit size with

$$k_x = k_y = 1 \quad , \quad \mathbf{u} = [1,1]^T \quad , \quad \nu = 1 \times 10^{10} \quad , \quad Q = 0 \tag{105}$$

The following Dirichlet boundary conditions are assumed

$\phi = 0$ along the boundary lines $x = 0$ and $y = 0$
$\phi = 100$ along the boundary line $x = 1$
$q_n = 0$ along the boundary line $y = 1$

The expected solution in this case is a uniform distribution of $\phi = 0$ over the whole domain except in the vicinity of the boundary $y = 1$ where a boundary layer is formed.

The domain has been discretized with a uniform mesh of 400 four node quadrilaterals as shown in Figure 8. Transverse stabilization effects have been accounted for choosing $\mathbf{v} = \boldsymbol{\nabla}\,\phi$ in eqn.(87). The initial values ${}^o\alpha_s^{(e)} = {}^o\alpha_t^{(e)} = 0$ have been taken in all elements.

Figure 9 shows the initial distribution of ϕ for $\alpha_s^{(e)} = \alpha_t^{(e)} = 0$ (standard Galerkin solution). Note the strong oscillations obtained as expected. The final converged solution for ϕ after 7 iterations is displayed in Figure 10 . Note that the boundary layer originated in the vicinity of the boundary at $y = 1$ is well reproduced with minimum oscillations. These oscillations grow considerably higher if the value of the transverse stabilization parameter $\alpha_t^{(e)}$ is kept equal to zero during the adaptive process, thus yielding the standard SUPG solution. A comparison of the distribution of ϕ along the center line obtained with the full

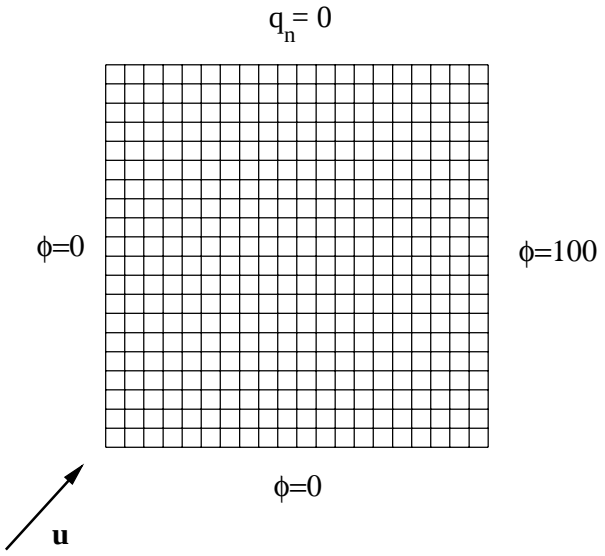

Figure 8: Two dimensional advection-diffusion problem with diagonal velocity. Finite element mesh of 400 linear quadrilaterals

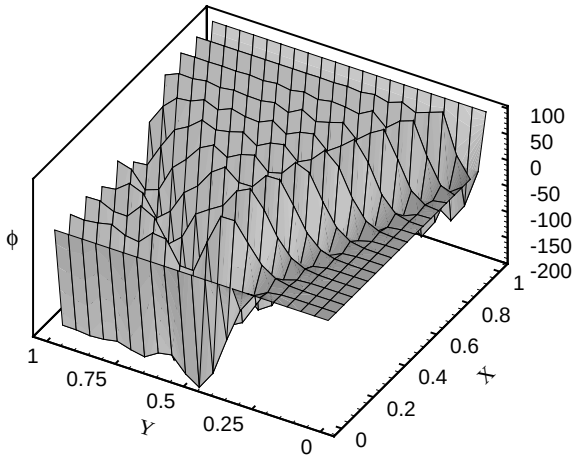

Figure 9: Two dimensional advection-diffusion problem with diagonal velocity. Initial oscillatory distribution of ϕ for $\alpha_s^e = \alpha_t^e = 0$.

stabilized approach (accounting for streamline and transverse stabilization effects) and the SUPG method is shown in Figure 11.

Figure 12 shows finally the smoothed distribution of the stabilization vector $\mathbf{h}$ given by eqn.(87). Note that in the central part of the domain the $\mathbf{h}$ vectors are aligned with the velocity direction (i.e. $h_t = 0$), whereas in the vicinity of the boundaries the effect of the transverse stabilization parameter h_t leads to a noticeable change of the direction of $\mathbf{h}$.

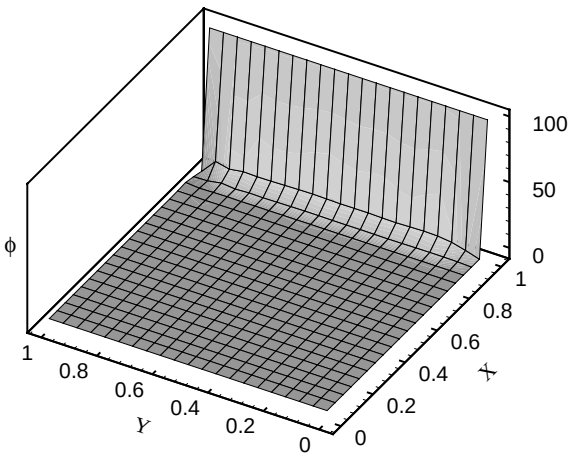

Figure 10: Two dimensional advection-diffusion problem with diagonal velocity. Final distribution of ϕ after 7 iterations.

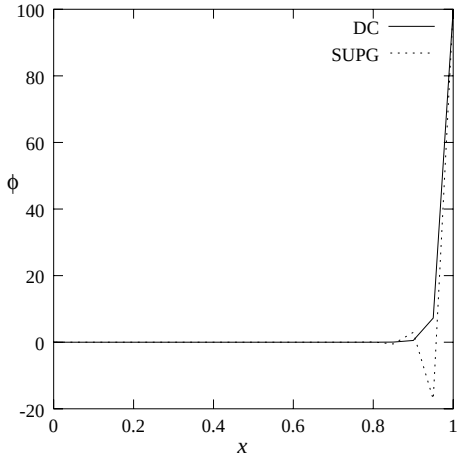

Figure 11: Two dimensional advection-diffusion problem with diagonal velocity. Distribution of ϕ along a center line obtained with the full stabilized discontinuity capturing method (DC) and the SUPG formulation ($\alpha_t = 0$)

5.4.2 Two dimensional advective-diffusive problem with no source and non uniform Dirichlet boundary conditions

The advection-diffusion equations are now solved with

$$\Omega =]-\frac{1}{2},\frac{1}{2}[\times]-\frac{1}{2},-\frac{1}{2}[\quad , \quad \mathbf{u} = [\cos\theta, -\sin\theta]^T \tag{106}$$

$$k_x = k_y = 10^{-6}, \quad Q(x,y) = 0, \quad \bar{\phi}(x,y) = \begin{cases} 100 & \text{if} \quad (x,y) \in \Gamma_{\phi_1} \\ 0 & \text{if} \quad (x,y) \in \Gamma_{\phi_2} \end{cases} \tag{107}$$

with $\Gamma_{\phi_1} = \{-1/2\} \times [1/4, 1/2] \cup]-1/2, 1/2[\times\{1/2\}$, $\Gamma_{\phi_2} = \Gamma_\phi - \Gamma_{\phi_1}$ and $\Gamma_q = 0$.

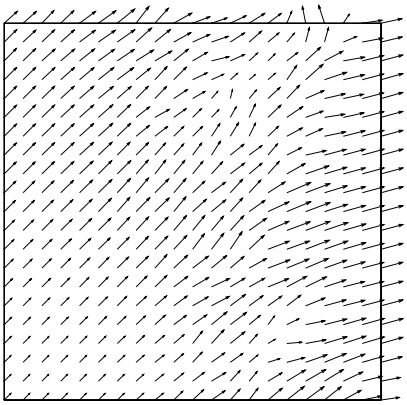

Figure 12: Two dimensional advection-diffusion problem with diagonal velocity. Final distribution of the stabilization vector $\mathbf{h}$.

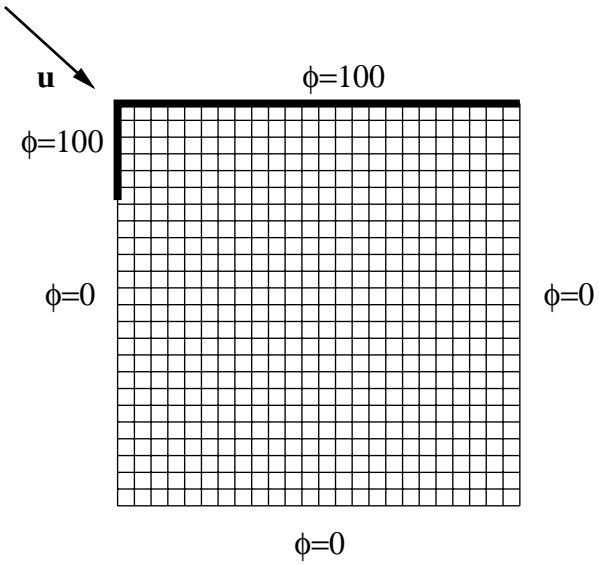

Figure 13: Two dimensional advection-diffusion problem with non uniform Dirichlet condition. Finite element mesh of 576 linear quadrilaterals

A structured mesh of 576 linear quadrangular has been chosen (Figure 13). The problem has been chosen for an angle of **u** given by $\tan\theta = 2$. Once again $\mathbf{v} = \boldsymbol{\nabla}\,\phi$ and the initial values ${}^{o}\alpha_s^{(e)} = {}^{o}\alpha_t^{(e)} = 0$ have been taken.

Figure 14 shows the oscillatory distribution of ϕ obtained for the first solution, as expected. The final distribution of ϕ after 7 iterations is displayed in Figures 15 and 16. Note that both the boundary layers at the edges and the internal sharp layer are captured with minor oscillations. These oscillations are more pronounced near the right hand side edge (Figure 16) when $\alpha_t^{(e)} = 0$ is taken through out the adaptive process (SUPG solution).

Figure 17 shows the distribution of the stabilization vector $\mathbf{h}$ of eqn.(87). Again note

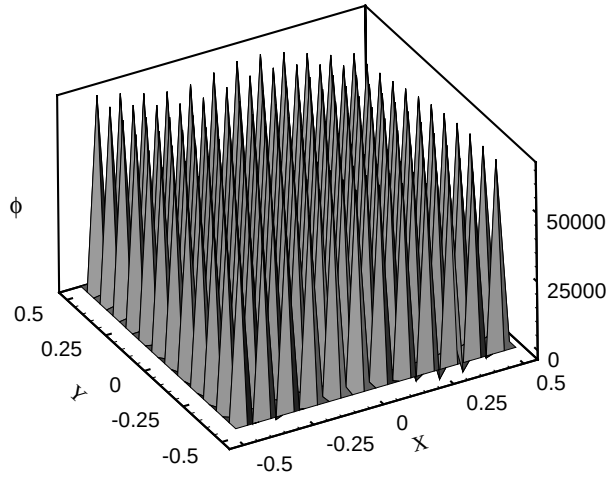

Figure 14: Two dimensional advection-diffusion problem with non uniform Dirichlet condition. Initial oscillatory distribution of ϕ for $\alpha_s^e = \alpha_t^e = 0$.

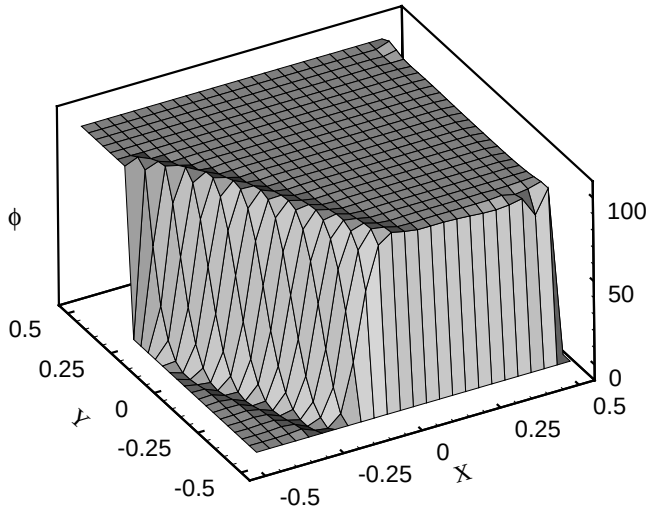

Figure 15: Two dimensional advection-diffusion problem with non uniform Dirichlet condition. Final distribution of ϕ after 7 iterations.

that the direction of $\mathbf{h}$ in the smooth part of the solution is aligned with that of the velocity vector, whereas the effect of the transverse stabilization term is very pronounced near the sharp gradient boundary regions. This leads to a change in the direction of $\mathbf{h}$ in these zones.

Other examples of application of the FIC procedure for computation of the stabilization parameter in 1D and 2D convection-diffusion problems can be found in.[36–39]

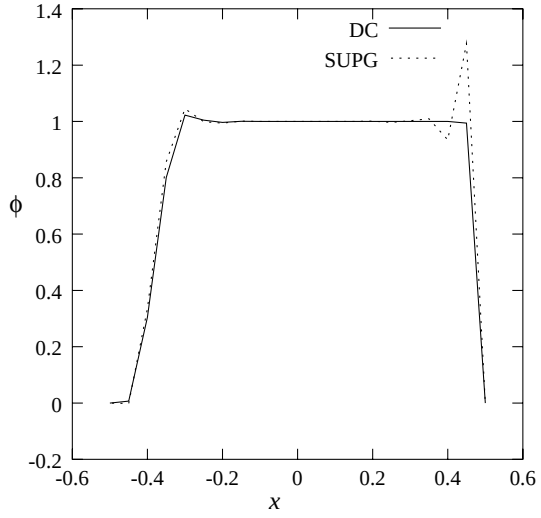

Figure 16: Two dimensional advection-diffusion problem with non uniform Dirichlet condition. Distribution of ϕ along a center line obtained with the full stabilized discontinuity capturing method (DC) and the SUPG formulation ($\alpha_t = 0$)

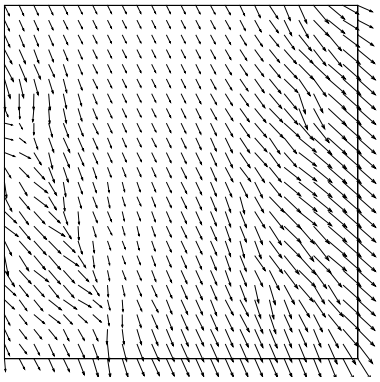

Figure 17: Two dimensional advection-diffusion problem with non uniform Dirichlet condition. Final distribution of the stabilization vector $\mathbf{h}$.

6 Stabilized space-time finite element formulation

Let us consider the balance of fluxes for the 1D advective-diffusive problem in an arbitrary finite space-tine slab $[x-h, x] \times [t-\delta, t]$ where h is the length of the space balance domain and δ is a time increment defining the size of the balance domain in the time axis (Figure 18). The global balance law can be written as

$$\int_{t-\delta}^{t} \left[\int_{x-h}^{x} f dx \right] dt = \int_{x-h}^{x} \left[\int_{t-\delta}^{t} \nu d\phi \right] dx \tag{108}$$

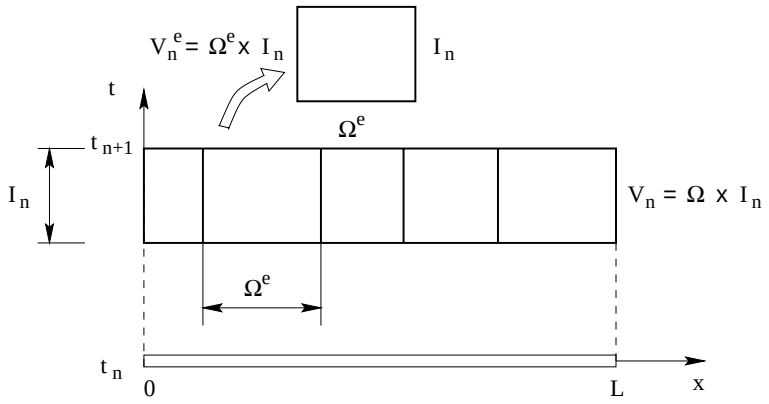

Figure 18: Space-time slab

where f denotes the space fluxes, ϕ is the transported variable and ν is the advective coefficient.

Assuming that both h and δ are finite and retaining first order terms in h and δ only gives[37,40]

$$r - \frac{h}{2}\frac{\partial r}{\partial x} - \frac{\delta}{2}\frac{\partial r}{\partial t} = 0 \qquad \text{for} \quad x \in]0, L[, \qquad t > 0 \tag{109}$$

with

$$r = -\left(\frac{\partial \phi}{\partial t} + u\frac{\partial \phi}{\partial x}\right) + \frac{\partial}{\partial x}\left(\kappa \frac{\partial \phi}{\partial x}\right) + Q \tag{110}$$

Eq. (109) can be considered the stabilized form of the balance differential equation for the transient 1D advective-diffusive problem. Note that for $h = \delta = 0$ the standard infinitesimal form of the transient advective-diffusive problem $r = 0$ is recovered. Eqn. (109) is also the basis for deriving numerical schemes ensuring the stability of the solution both in space and time domains. Note that in all cases the distance h and the time increment δ in (109) play the role of stabilization parameters ensuring stability of the numerical solution for the discrete problem. Indeed the correct evaluation of these parameters is critical and this issue will be discussed in a next section for the space-time formulation.

6.1 Equivalence of the FIC method with the Lax-Wendrof and Characteristic Galerkin formulation

Let us consider the stabilized transient equations (109) neglecting for simplicity the term involving the time stabilization parameter δ. A forward Euler integration gives

$$\Delta\phi = \Delta t[\bar{r} - \tau u \frac{\partial \bar{r}}{\partial x}]^n \tag{111}$$

where as usual the intrinsic time $\tau = \frac{h}{2|u|}$ and $\bar{r}$ is the steady state "residual" defined as

$$\bar{r} = -u\frac{\partial \phi}{\partial x} + \frac{\partial}{\partial x}\left(k\frac{\partial \phi}{\partial x}\right) + Q \tag{112}$$

The well known Lax-Wendroff approximation is written as[52]

$$\Delta\phi = \Delta t \left[\bar{r} - \frac{\Delta t}{2} u \frac{\partial \bar{r}}{\partial x} \right]^n \tag{113}$$

The equivalence between eqns. (111) and (113) is obvious if the time increment Δt within the brackets in eqn. (113) is taken to coincide with the parameter τ. Recall that eq. (113) is identical to that found using the Taylor-Galerkin method.[4,25,37] The analogy with the FIC method also applies in this case.

The same analogy can be found between the FIC method and the so called characteristic formulation for 2D/3D problems.[4,26] The analogous expressions are[37]

FIC method	**Characteristic approximation**
$\Delta\phi = \Delta t[\bar{r} - \tau \mathbf{u}^T \boldsymbol{\nabla}\, \bar{r}]$	$\Delta\phi = \Delta t[\bar{r} - \frac{\Delta t}{2} \mathbf{u}^T \boldsymbol{\nabla}\, \bar{r}]$

(114)

Applications of the Galerkin FEM technique to above equations leads to analogous stabilized FEM schemes.

6.2 Stabilized space-time FEM formulation

Let us consider next in more detail the so called space-time (discontinuous) FEM formulation.

Let us transform the time "direction" t into an auxiliary "spatial" direction y^* by means of a fictitious "time velocity" v^* so that

$$y^* = v^* t \tag{115}$$

Using this concept eqn. (109) can be rewritten as

$$r - \frac{1}{2} \mathbf{h}^T \boldsymbol{\nabla} r = 0 \qquad \text{for} \quad x \in]0, L[, \qquad y^* > 0 \tag{116a}$$

where

$$r = -\boldsymbol{\nabla}^T \mathbf{f} + \boldsymbol{\nabla}^T \mathbf{D} \boldsymbol{\nabla} \phi + Q \tag{116b}$$

the advective flux vector is

$$\mathbf{f} = [u\phi, v^* \phi]^T \tag{116c}$$

$$\boldsymbol{\nabla} = \left[\frac{\partial}{\partial x}, \frac{\partial}{\partial y^*} \right]^T \quad , \quad \mathbf{D} = \begin{bmatrix} \kappa & 0 \\ 0 & 0 \end{bmatrix} \tag{116d}$$

The *characteristic length* vector $\mathbf{h}$ is given by

$$\mathbf{h} = [h, \delta v^*]^T \tag{117}$$

and the "intrinsic time" of the space-time problem can be defined now as

$$\tau = \frac{\bar{h}}{2|\mathbf{u}|} \tag{118}$$

where the characteristic length $\bar{h}$ is

$$\bar{h} = [h^2 + (\delta v^*)^2]^{1/2} \tag{119a}$$

and

$$|\mathbf{u}| = [u^2 + (v^*)^2]^{1/2} \quad \text{with } \mathbf{u} = \left\{ \begin{array}{c} u \\ v^* \end{array} \right\} \tag{119b}$$

In the following it will be assumed that the characteristic length vector is aligned with the velocity vector. This implies

$$\mathbf{h} = \frac{\bar{h}}{|\mathbf{u}|}\mathbf{u} = 2\tau\mathbf{u} \tag{120}$$

Above assumption is the basis of a kind of streamline-upwinding approach for the transient problem,[40] where the so called "artificial" or numerical dissipation is introduced along the streamlines direction only. Indeed, this assumption is not mandatory and other more advantageous options are possible as mentioned for the steady-state case.

Substituting eqn. (120) into (116a) gives the alternative form of the stabilized space-time differential equation in terms of the intrinsic time parameter as

$$r - \tau\mathbf{u}^T\boldsymbol{\nabla}r = 0 \tag{121}$$

The equivalent stabilized form (121) has to be solved together with the following boundary conditions

$$\phi - \bar{\phi} = 0 \quad \text{on } \Gamma_\phi \tag{122a}$$

$$\mathbf{n}^T\mathbf{D}\boldsymbol{\nabla}\phi + \bar{q} - \tau\mathbf{u}^T\mathbf{n}r = 0 \quad \text{on } \Gamma_q \tag{122b}$$

$$\phi(\mathbf{x}, 0) = \bar{\phi}_0 \quad \text{for } t = t_0 \tag{122c}$$

In above Γ_ϕ and Γ_q are the usual space boundaries, where the variable and the normal flux are prescribed, respectively, $\mathbf{n}$ is the normal vector, $\bar{q}$ is the prescribed normal flux at the Neumann boundary Γ_q, $\bar{\phi}$ is the prescribed value of the unknown at the Dirichlet boundary Γ_ϕ and $\bar{\phi}_0$ is the known value of ϕ at the initial time.

Note that eqn. (122b) is obtained substituting the value of $\mathbf{h}$ from eqn. (120) into (78c).

6.2.1 Finite element approximation

Consider the partition $0 = t_0 < t_1 \ldots < t_n = T$ of the time interval $I =]0, T[$. Denote by $I_n =]t_n, t_{n+1}[$ the nth time interval. A space-time slab is defined as

$$V_n = \Omega \times I_n \tag{123}$$

where $\Omega(=]0, L[)$ denotes the space domain (Figure 18). Indeed using eqn. (115) the equivalent partition $0 = y_0^* < y_1^* \ldots < y_n^*$ can be defined.

For the nth space-time slab, let the space domain be subdivided into n_e elements, $\Omega^e,\ e = 1, \ldots n_e$. The space-time element domains are defined as

$$V_n^e = \Omega^e \times I_n, \qquad e = 1, \ldots, n_e \tag{124}$$

Within each space-time element containing n nodes the finite element approximation is written as

$$\phi \simeq \hat{\phi} = \sum_{i=1}^{n} N_i(x, y^*)\phi_i \tag{125}$$

where N_i are the element shape functions and ϕ_i are nodal values. The functions N_i are assumed C^0 continuous throughout each space-time slab, but are allowed to be discontinuous across the slab interfaces, namely at times $t_1, t_2, \ldots, t_{N-1}$ (or the equivalent time "coordinates" $y_1^*, y_2^*, \ldots y_{N-1}^*$). Substituting eqn. (125) into (121) and (122b) gives

$$\hat{r} - \tau \mathbf{u}^T \boldsymbol{\nabla} \hat{r} = r_V \quad \text{on } V_n \tag{126a}$$

$$-\mathbf{n}^T \mathbf{u} \hat{\phi} + \mathbf{n}^T \mathbf{D} \boldsymbol{\nabla} \hat{\phi} + \bar{q} - \tau \mathbf{u}^T \mathbf{n} \hat{r} = r_q \quad \text{on } \Gamma_q \tag{126b}$$

where $\hat{r} = r(\hat{\phi})$ and r_V and r_q are the residuals of the approximate solution in the space-time slab V_n and the Neumann boundary Γ_q, respectively. As usual in the FEM, the Dirichlet boundary condition (122a) will be assumed to be satisfied exactly.

The weighted residual form of eqns. (126) is

$$\int_{V_n} w(\hat{r} - \tau \mathbf{u}^T \boldsymbol{\nabla} \hat{r}) dV + \int_{\Gamma_q} \bar{w} [\mathbf{n}^T \mathbf{D} \boldsymbol{\nabla} \hat{\phi} + \bar{q} - \tau \mathbf{u}^T \mathbf{n} \hat{r}] d\Gamma_n = 0 \tag{127}$$

where w and $\bar{w}$ are arbitrary test functions with the same continuity properties that the shape functions. As usual $w = \bar{w} = 0 \quad$ on Γ_ϕ will be assumed. Integrating by parts the term incorporating τ in the first integral of eqn. (127) and choosing $\bar{w} = -w$ gives

$$\int_{V_n} \left[w + \boldsymbol{\nabla}^T (\tau \mathbf{u} w) \right] \hat{r} dV - \int_{\Gamma_q} w(\mathbf{n}^T \mathbf{D} \boldsymbol{\nabla} \hat{\phi} + \bar{q}) d\Gamma_n = 0 \tag{128}$$

Let us further assume that both the intrinsic time and the velocity are constant within each element (i.e. $\boldsymbol{\nabla}^T \tau \mathbf{u} = 0$). Integrating by parts the diffusive terms in the product $w\hat{r}$ within the first integral of eq. (128) gives

$$\begin{aligned} &\int_{V_n} [w \boldsymbol{\nabla}^T \mathbf{f} + (\boldsymbol{\nabla}^T w) \mathbf{D} \boldsymbol{\nabla} \hat{\phi} - wQ] dV + \sum_e \int_{V_n^e} \tau \mathbf{u}^T \boldsymbol{\nabla} w [\nu \boldsymbol{\nabla}^T \mathbf{f} - \\ &- \boldsymbol{\nabla}^T (\mathbf{D} \boldsymbol{\nabla} \hat{\phi}) - Q] dV + \int_{\Gamma_q} w \bar{q} d\Gamma_n = 0 \end{aligned} \tag{129}$$

Let us compute the integral along the Neumann boundaries Γ_{q_n} in eqn. (129) for the space-time slab of Figure 19. The total flux is the sum of the advective and diffusive fluxes across the lateral boundaries Γ_L and Γ_R and the advective flux across the lower boundary Γ_n^+ and the upper boundary Γ_{n+1}^-.

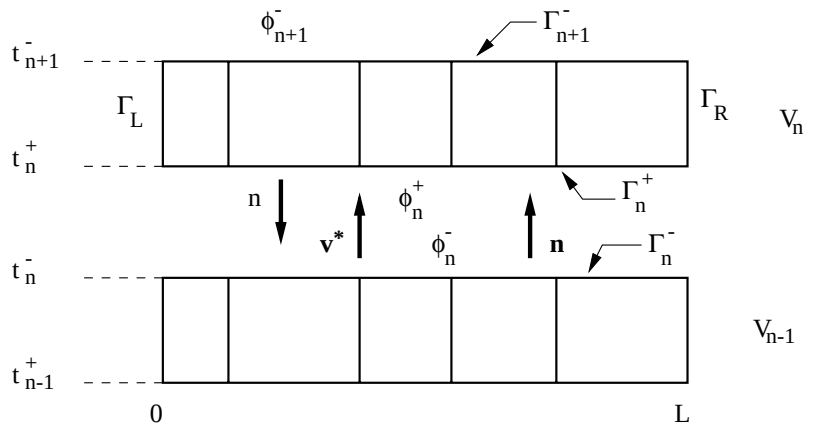

Figure 19: Space-time slab. Definition of Neumann boundaries where the flux is prescribed

The normal flux $\bar{q}$ on the lower and upper boundaries Γ^+_n and Γ^-_{n+1} can be computed from the advective velocity v^* as

$$\begin{aligned} \bar{q} &= -v^*\phi^-_n \qquad \text{on} \quad \Gamma^+_n \\ \bar{q} &= v^*\phi^+_{n+1} \qquad \text{on} \quad \Gamma^-_{n+1} \end{aligned} \tag{130}$$

Introducing eqns. (130) into the third integral in eqn. (129) gives

$$\int_{\Gamma_q} w\bar{q}d\Gamma = \int_{\Gamma^+_n} wv^*(\phi^+_n - \phi^-_n)dx + \int_{\Gamma^-_{n+1}} wv^*(\phi^+_{n+1} - \phi^-_{n+1})\,dx + \int_{\Gamma_{R+L}} w\bar{q}dt \tag{131}$$

The first integral of the r.h.s. of eqn. (131) gives the so called jump conditions in a discontinuous approximation in time of the unknown ϕ. The second integral can be set equal to zero by assuming $\phi^-_{n+1} = \phi^+_{n+1}$ while solving the equations for the time slab. Using this later assumption and substituting eqn. (131) into (129) gives the final expression for the stabilized integral form as

$$\begin{aligned} &\int_{V_n} [w\nu\boldsymbol{\nabla}^T\mathbf{f} + (\boldsymbol{\nabla}^T w)\mathbf{D}\boldsymbol{\nabla}\hat{\phi} - wQ]dV + \\ &\quad + \sum_e \int_{V^e_n} \tau\mathbf{u}^T\boldsymbol{\nabla}w[\nu\boldsymbol{\nabla}^T\mathbf{f} - \boldsymbol{\nabla}^T(\mathbf{D}\boldsymbol{\nabla}\hat{\phi}) - Q]dV + \\ &\quad + \int_{\Gamma^+_n} wv^*(\phi^+_n - \phi^-_n)dx + \int_{\Gamma_{R+L}} w\bar{q}dt = 0 \end{aligned} \tag{132}$$

The first and fourth integrals in eqn. (132) constitute the standard Galerkin formulation. The second integral introduces the stabilization terms arising naturally from the FIC formulations. Note the equivalence of these terms with an analogous SUPG space-time formulation.[27] The third integral is the standard jump condition derived from the lack of continuity of the unknown variable across the upper and lower slab interfaces. The jump condition imposes a weakly enforced continuity across these interfaces and is the mechanism by which

information is propagated from one space-time slab to another. Eqn. (132) leads to a discretized system of equations where the unknowns are the nodal values of ϕ_n^+ and ϕ_{n+1}^- at the boundaries Γ_n^+ and Γ_{n+1}^-, respectively (see Figure 19).

The choice of a *continuous* approximation in time leads to the same stabilized expression (132), where the third integral imposing slab continuity now vanishes. Naturally in this case the discretized system involves the nodal unknowns for the whole space-time domain.

6.2.2 Computation of the stabilization parameter in the space-time formulation

The method to compute the stabilization parameter in the space-time FEM formulation is an extension of the approach proposed for steady state problems in Section 5.2.2. Following the same arguments of Sections 5.2.2 and 5.2.3 lead to the same expression for the intrinsic time of a space-time element as

$$\tau^{(e)} \geq (r_2^{(e)} - r_1^{(e)})[(\mathbf{u}^T \boldsymbol{\nabla} \hat{r}_2)^{(e)} - (\mathbf{u}^T \boldsymbol{\nabla} \hat{r}_1)^{(e)}]^{-1} \tag{133}$$

The following iterative scheme can be now implemented to compute the intrinsic time parameter in order to obtain a stable numerical solution both in space and time.

1. Solve the stabilized problem defined by eqns. (121) and (122) to find ϕ_n^+ and ϕ_{n+1}^- with an initial guess of $\tau^{(e)} = {}^0\tau_n^{(e)}$. In the examples shown next ${}^0\tau_n^{(e)} = \tau_{n-1}^{(e)}$ (with $\tau_1^{(e)} = 0$) has been chosen. Compute $r_1^{(e)}$ and $\boldsymbol{\nabla} r_1^{(e)}$.

2. Compute an enhanced solution. In the examples shown the enhanced spatial derivative field has been obtained both in space and time by simple nodal averaging of element derivatives over two space-time elements. For this purpose the following value of the nodal unknown at time t_n is used

$$\phi_n = \frac{1}{2}(\phi_n^- + \phi_n^+) \tag{134}$$

3. Compute $r_2^{(e)}$ and $\boldsymbol{\nabla} r_2^{(e)}$.

4. Compute a new value for the element intrinsic time ${}^1\tau_n^{(e)}$ using eqn. (133).

5. Compute a new value of $\tau^{(e)}$ by $\tau^{(e)} = ({}^1\tau_n^{(e)} - {}^0\tau_n^{(e)})\beta + {}^0\tau^{(e)}$, where β is a relaxation parameter. In the examples solved $\beta = 0.8$ has been taken.

6. Repeat steps 1-5 using the updated intrinsic time values until convergence for $\tau^{(e)}$ is found or else a satisfactory numerical solution is obtained.

Steps 1-6 are repeated for each time step. In the examples solved it has been found useful to smooth the distribution of the ${}^i\tau^{(e)}$ values obtained after Step 5. This has been simply done again by nodal averaging. It is also noted that above iterative process converges quite fast for well developed transient solutions (error in quadratic norm for ${}^i\tau^{(e)}$ less than 1 % obtained in 2-3 iterations) as the initial guess for $\tau^{(e)}$ is taken as the converged value from previous time step. The convergence in the first time step can be accelerated by using for ${}^0\tau^{(e)}$ the critical value from the simple steady state sourceless advective-diffusive case solved with linear elements, i.e. $\tau^{(e)} = \frac{l^{(e)}}{2u}\left(1 - \frac{1}{\gamma^{(e)}}\right)$ with the Peclet number $\gamma^{(e)} = \frac{ul^{(e)}}{2\kappa}$.

7 Examples of stabilized transient solution using the FIC method

7.1 Transient convection-diffusion problem with linear initial distribution

The first example solves the convection-diffusion problem

$$\frac{\partial \phi}{\partial t} + u\frac{\partial \phi}{\partial x} - k\frac{\partial^2 \phi}{\partial x^2} = 0 \tag{135}$$

with the initial and boundary conditions

$$\begin{aligned} \phi(x, t_0) &= x \\ \phi(0, t) &= 0 \\ \phi(L, t) &= 1 \end{aligned} \tag{136}$$

is presented. The data of the problem are $L = 1$, $u = 1$, $k = 0.01$. The discretization in the space-time domain has been carried out using twenty four node bilinear square elements with dimensions in space and time equal to 0.05. Two time steps have been used for the simulations: $\Delta t = 0.05$ and $\Delta t = 0.1$. Using eqn. (115) the "time velocities" are respectively $v^* = 1$ and $v^* = 0.5$. The resulting element Peclet number is 2.5 and the Courant numbers (defined as $C = \frac{|u|\Delta t}{l^e}$) for the two cases considered are respectively $C = 1$ and $C = 2$.

The numerical results are presented in Figures 20 to 23. In Figures 20 and 22 the value of ϕ is plotted at times from 0 to 4 in steps of 0.5 obtained with (a) the automatic computation of the stabilization parameter τ using the iterative adaptive scheme described in previous sections, (b) using the standard non-stabilized Galerkin method and (c) using the expression for τ given by Shakib[53]

$$\tau = [(2u/\Delta x)^2 + (4k/\Delta x^2)^2]^{-1/2} \tag{137}$$

where Δx is the spatial element length.

As expected the Galerkin method lacks stability in both cases, producing spurious oscillations at all time steps, including the stationary state. On the other hand the solution utilizing the stabilization parameter given by eqn. (137) shows a higher diffusivity, failing to reach the correct solution at steady state. The proposed method stabilizes the solution, and seems to give the correct distribution of ϕ at all times.

The time evolution of τ is represented in Figures 20d and 21d ($C = 1$) and 22d and 23d and ($C = 2$). Note that, the distribution is not constant over the spatial domain, specially at the early stages of the analysis. The optimal steady state value for the SUPG formulation ($\tau = 0.015$) is reached in both cases.

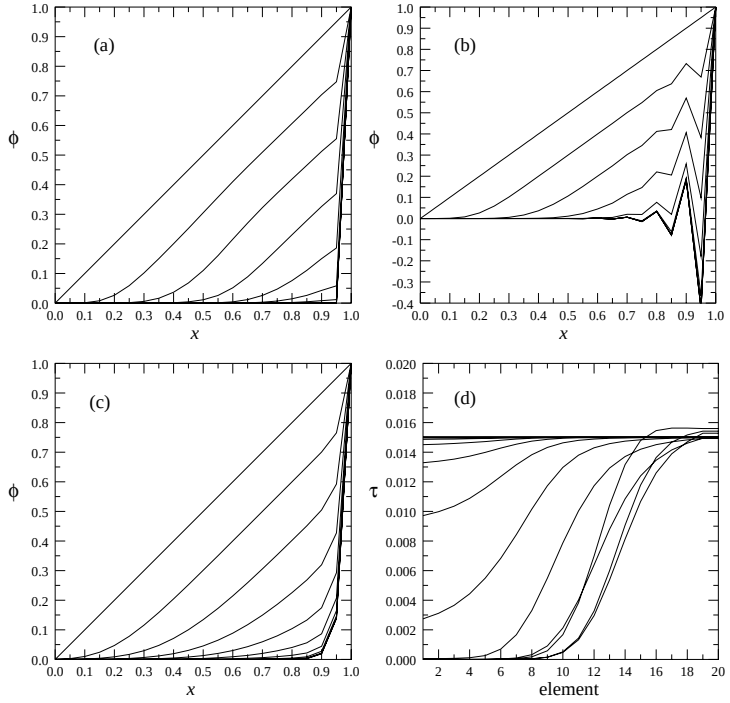

Figure 20: Solution of the advection diffusion problem with $C = 1$, using (a) automatic computation of τ, (b) Galerkin method, (c) τ as defined by eqn. (137), (d) time evolution of the distribution of τ as obtained with the present method.

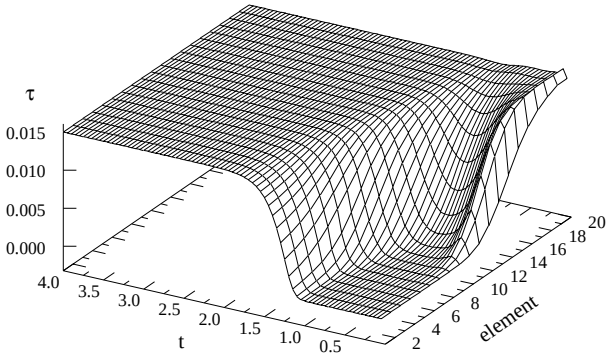

Figure 21: Solution of the advection diffusion problem with $C = 1$. Time evolution of the stabilization parameter τ for each element.

7.2 Burger's equation

In this example the method derived for the advection diffusion equation is applied to the non linear Burgers equation

$$\frac{\partial \phi}{\partial x} + \phi \frac{\partial \phi}{\partial x} - k \frac{\partial^2 \phi}{\partial x^2} = 0 \tag{138}$$

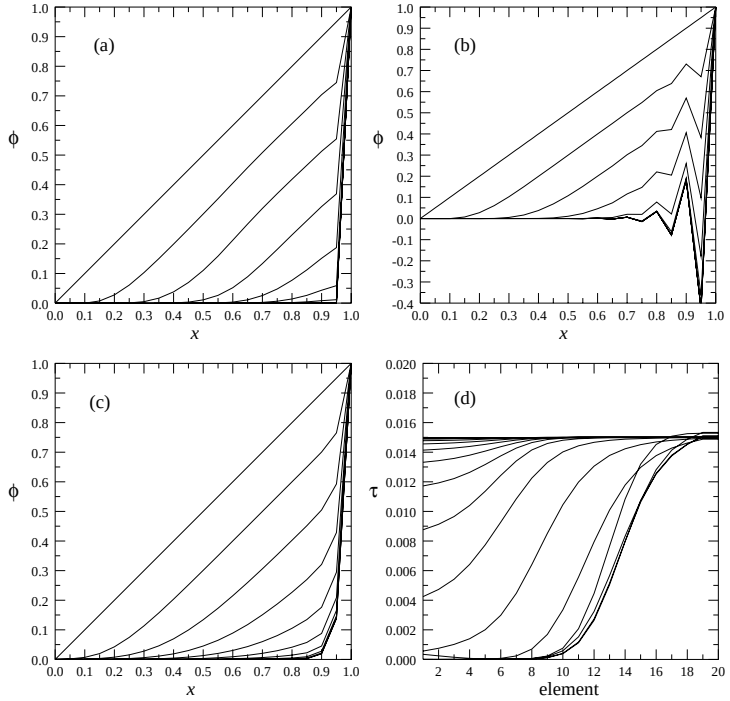

Figure 22: Solution of the advection diffusion problem with $C = 2$, using (a) automatic computation of τ, (b) Galerkin method, (c) τ as defined by eqn. (137), (d) time evolution of the distribution of τ as obtained with the present method.

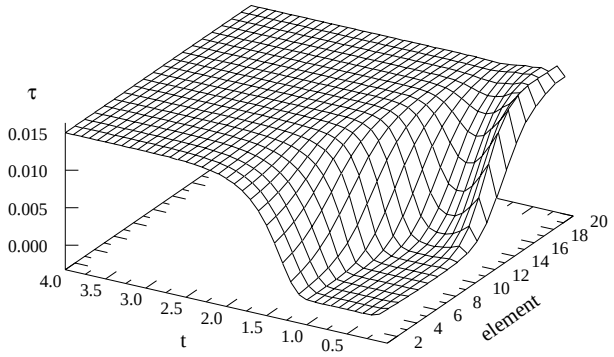

Figure 23: Solution of the advection diffusion problem with $C = 2$. Time evolution of the stabilization parameter τ for each element.

with the initial and boundary conditions

$$\begin{aligned} \phi(x, t_0) &= \sin \pi x \\ \phi(0, t) &= 0 \\ \phi(L, t) &= 0 \end{aligned} \tag{139}$$

with $k = 1/100\ \pi$. The discretization of the space time domain has been carried out using 80 equally spaced four nodal rectangular elements. The dimension in space is $\Delta x = 0.0125$ and the dimension in time is $\Delta y = 1$. The time step has been taken as $\Delta t = 4.67 \times 10^{-3}$. The "space velocity" is therefore $v^* = 214.13$.

The numerical solution is shown in Figure 24 at times from 0 to 0.7 for $\Delta t = 0.14$ using the different methods described in Example 7.1. As for the previous examples the solution develops smoothly during the initial time steps, thus even the standard Galerkin solution does not show any spurious oscillation. Again unsatisfactory results are evident only when the maximum value reaches the right boundary (Figure 24(b)).

The results obtained using the parameter τ as defined by eqn. (137) prove again to be over diffusive, specially when the solution is smooth (Figure 24(c)). The solution obtained with the automatic parameter computation based on the FIC method are smooth and less diffusive for all time steps.

The space time distribution of τ depicted in Figure 24(d) and 25 reveals that the stabilization parameter has a significant value only for the elements that show a lack of stability in the Galerkin solution.

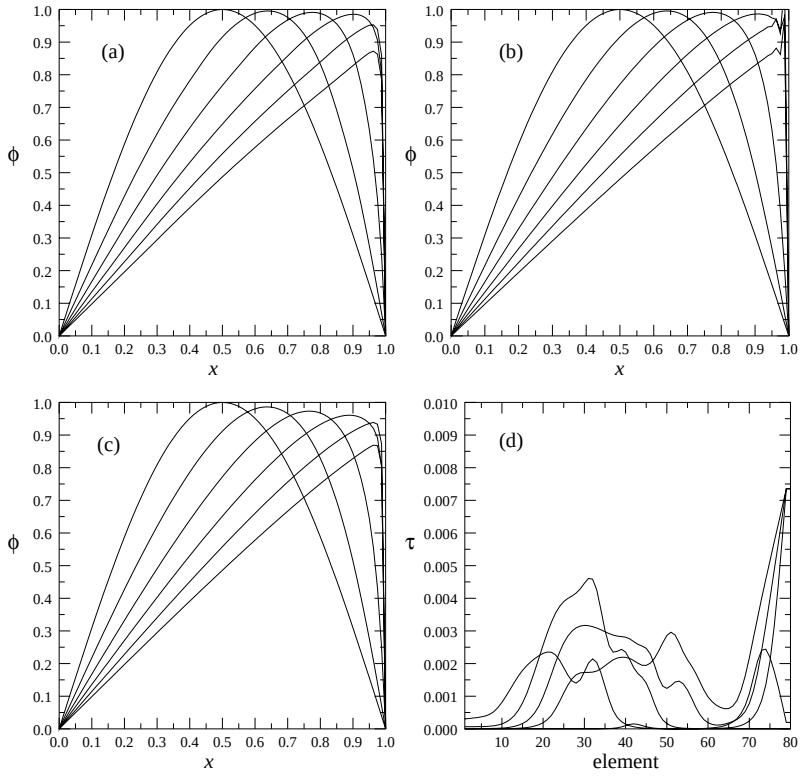

Figure 24: Solution of the Burgers equation with $C = 2$, using (a) automatic computation of τ, (b) Galerkin method, (c) τ as defined by eqn. (137), (d) time evolution of the distribution of τ as obtained with the present method.

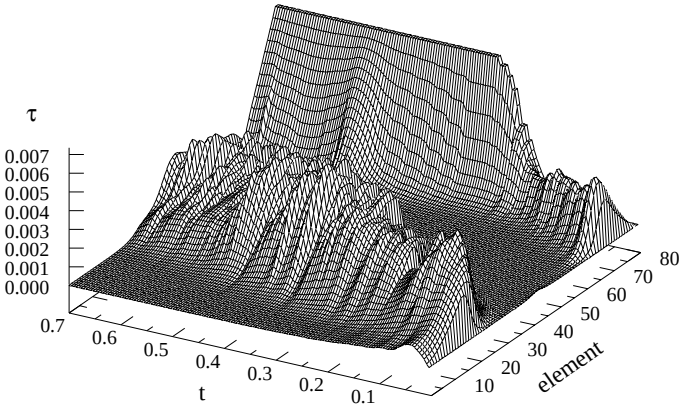

Figure 25: Solution of the Burgers equation with $C = 2$. Time evolution of the stabilization parameter τ for each element.

8 CONCLUDING REMARKS

A review of some of the more popular procedures for deriving stable finite element formulation for solving the convective-diffusion equation has been presented. It has been shown that most methods can be derived as particular cases of the so called Finite Increment Calculus (FIC) procedure based on the solution of modified governing equations obtained using higher order balance laws. The FIC method also provides a methodology for computing the streamline and cross-wind stabilization parameters. The efficiency of the FIC approach has been shown in the finite element solution of steady-state and transient convection-diffusion problems.

References

[1] S.V. Patankar, *Numerical Heat Transfer and Fluid Flow (Series in Computational Methods in Mechanics and Thermal Sciences)*, ed. Minkowycz, W.J. & Sparrow, E.M., Hemisphere, Washington, 1980.

[2] C. Hirsch, "*Numerical computations of internal and external flow*", John Wiley, Vol. 1, 1988; Vol. 2, 1990.

[3] S. Idelsohn and E. Oñate, "Finite element and finite volumes. Two good friends", *Int. J. Num. Meth. Engng.*, Vol. **37**, 3323–3341, 1994.

[4] O.C. Zienkiewicz and R.L. Taylor, "*The finite element method*", Mc.Graw Hill, Vol. I., 1989, Vol. II., 1991.

[5] E. Oñate, S. Idelsohn, O.C. Zienkiewicz and R.L. Taylor, "A finite point method in computational mechanics. Applications to convective transport and fluid flow", *Int. J. Num. Meth. Engng.*, **39**, 3839–3866, 1966.

[6] E. Oñate, S. Idelsohn, O.C. Zienkiewicz, R.L. Taylor and C. Sacco, "A stabilized finite point method for fluid mechanics", *Comp. Meth. Appl. Mech. Engng.*, **139**, 315–247, 1996.

[7] E. Oñate and S. Idelsohn, "A mesh free finite point method for advective-diffusive transport problems", *Comput. Mechanics*, **21**, 283–292, 1988.

[8] I. Christie, D. Griffiths, A.R. Mitchell and O.C. Zienkiewicz, "Finite element methods for second order differential equations with significant first derivatives", *Int. J. Num. Meth. Engng.*, **10**, 1389–96, 1976.

[9] J.C. Heinrich, P.S. Hayakorn and O.C. Zienkiewicz, "An upwind finite element scheme for two dimensional convective transport equations", *Int. J. Num. Meth. Engng.*, **11**, 131–143, 1977.

[10] D.W. Kelly, S. Nakazawa, O.C. Zienkiewicz and J.C. Heinrich, "A note on upwind and anisotropic balancing dissipation in finite element approximation to convective diffusion problems", *Int. J. Num. Meth. Engng.*, **15**, 1705–1711, 1980.

[11] J.C. Heinrich, "On quadratic elements in finite element solutions of steady state convection-diffusion equations", *Int. J. Num. Meth. Engng.*, **15**, 11041–1052, 1980.

[12] A.N. Brooks and T.J.R. Hughes, "Streamline Upwind/Petrov-Galerkin formulations for convective dominated flows with particular emphasis on the incompressible Navier-Stokes equations", *Comput. Meth. in Appl. Mech. and Engng.* , **32**, 199-259, 1982.

[13] T.E. Tezduyar and D.K. Ganjoo, "Petrov-Galerkin Formulations with weighting functions dependent upon spatial and temporal discretization: Applications to transient convection-diffusion problems", *Comput. Meths. Appl. Mech. Engrg*, **59**, 49-71, 1986.

[14] T.J.R. Hughes and M. Mallet, "A new finite element formulations for computational fluid dynamics: III. The generalized streamline operator for multidimensional advective-diffusive systems", *Comp. Meth. Appl. Mech. Engng.*, **58**, 305–328, 1986.

[15] C.C. Yu and J.C. Heinrich, "Petrov-Galerkin method for multidimensional time dependent convection-diffusion equations", *Int. J. Num. Meth. Engngn.*, **24**, 2201–2215, 1987.

[16] S.R. Idelsohn, "Upwind techniques via variational principles", *Int. J. Num. Meth. Engng.*, **28**, 769–84, 1989.

[17] L. Franca, S. Frey, and T.J.R. Hughes, "Stabilized finite element methods: I. Application to the advective-diffusive model", *Comput. Meths. Appl. Mech. Engrg*, **95**, pp. 253-276, 1992.

[18] R. Codina, E. Oñate, and M. Cervera, "The intrinsic time for the SUPG formulation using quadratic elements", *Comput. Meths. Appl. Mech. Engrg*, **94**, 239-262, 1992.

[19] R. Codina, "A finite element formulation for the numerical solution of the convection-diffusion equation", *publication CIMNE*, **14**, 1993.

[20] J.C. Heinrich, S.R. Idelsohn, E. Oñate and C.A. Vionnet, "Boundary conditions for finite element simulation of convective flows with artificial boundaries", *Int. J. Num. Meth. Engngn.*, **39**, 1053–71, 1996.

[21] S.R. Idelsohn, J.C. Heinrich and E. Oñate, "Petrov-Galerkin methods for the transient advective-diffusive equation with sharp gradients", *Int. J. Num. Meth. Engngn.*, **39**, 1455–73, 1996.

[22] R. Codina, comparison of some finite element methods for solving the diffusion-convection-reaction equation, *Comput. Meths. Appl. Mech. Engrg*, **156**, pp. 185-210, 1998.

[23] J. Donea, T. Belytschko and P. Smolinski, "A generalized Galerkin method for steady state convection-diffusion problems with applications to quadratic shape functions elements", *Comp. Meth. Appl. Mech. Engng.*, **48**, 25–43, 1985.

[24] M.B. Goldschmit and E.N. Dvorkin, "On the solution of the steady-state convection-diffusion equation using quadratic elements. A generalized Galerkin technique also reliable with distorted meshes", *Engng. Comput.*, **11**, 6, 565–579, 1994.

[25] J. Donea, "A Taylor-Galerkin method for convective transport problems", *Int. J. Num. Meth. Engng.*, **20**, 101–119, 1984.

[26] O.C. Zienkiewicz and R. Codina, "A general algorithm for compressible and incompressible flow. Part I: the split, characteristic based scheme", *Int J, Num., Meth. Fluids* , **20**, 869-885, 1995.

[27] T.J.R. Hughes, L.P. Franca and G.M. Hulbert, "A new finite element formulation for computational fluid dynamics: VIII. The Galerkin/least-squares method for advective-diffusive equations", *Comput. Meth. in Appl. Mech. Engng.* , **73**, 173-189, 1989.

[28] L.P. Franca, S.L. Frey and T.J.R. Hughes, "Stabilized finite element methods: I. Application to the advective-diffusive model", *Comput. Meth. Appl. Mech. Engn*, Vol. **95**, pp. 253–276, 1992.

[29] T.J.R. Hughes, "Multiscale phenomena: Green's function, the Dirichlet-to-Neumann formulation, subgrid scale models, bubbles and the origin of stabilized formulations", *Comput. Meth. in Appl. Mech. and Engng.* , **127**, 387-401, 1995.

[30] F. Brezzi, L.P. Franca, T.J.R. Hughes and A. Russo, "$b = \int g$", *Comput. Meth. Appl. Mech. Engn.*, **145**, 329–339, 1997.

[31] T.J.R. Hughes, G.R. Feijoo, L.Mazzei and J.B. Quincy, "The variational multiscale method: A paradigm for computational mechanics", *Comput. Meth. Appl. Mech. Engn*, Vol. **166**, 3–24, 1998.

[32] F. Brezzi, M.O. Bristeau, L.P. Franca, M. Mallet and G. Rogé, "A relationship between stabilized finite element methods and the Galerkin method with bubble functions", *Comput. Meth. Appl. Mech. Engn.*, Vol. **96**, 117–129, 1992.

[33] L.P. Franca and C. Farhat, "Bubble functions prompt unusual stabilized finite element methods", *Comput. Meth. in Appl. Mech. and Engng.* , **123**, 299-308, 1994.

[34] F. Brezzi, D. Marini and A. Russo, "Pseudo residual-free bubbles and stabilized methods", *Computational Methods in Applied Sciences '96*, J. Periaux *et. al.* (Eds.), J. Wiley, 1996.

[35] F. Brezzi, D. Marini and A. Russo, "Applications of the pseudo residual-free bubbles to stabilization of convection-diffusion problems", *Comput. Meths. Appl. Mech. Engrg*, **166**, 51-63, 1998.

[36] E. Oñate, "Derivation of stabilized equations for numerical solution of advective-diffusive transport and fluid flow problems", *Comput. Meth. in Appl. Mech. Engng.* , **151**, 233-265, 1998.

[37] E. Oñate, J. García and S. Idelsohn, "Computation of the stabilization parameter for the finite element solution of advective-diffusive problems", *Int. J. Num. Meth. Fluids*, Vol. **25**, 1385–1407, 1997.

[38] E. Oñate, J. García and S. Idelsohn, "An alpha-adaptive approach for stabilized finite element solution of advective-diffusive problems with sharp gradients", *New Adv. in Adaptive Comp. Met. in Mech.*, P. Ladeveze and J.T. Oden (Eds.), Elsevier, 1998.

[39] J. García, "Finite element analysis of ship hydrodynamic problems", Ph.D. Thesis (in Spanish), Univ. Politécnica de Cataluña, Barcelona, 1999.

[40] E. Oñate and M. Manzan, "A general procedure for deriving stabilized space-time finite element methods for advective-diffusive problems", *Int. J. Numer. Meth. Fluids*, **31**, 203-221,1999.

[41] R. Courant, E. Isaacson and M. Rees, "On the solution of non-linear hyperbolic differential equations by finite differences", *Comm. Pure Appl. Math.*, **V**, 243–55, 1952.

[42] D.B. Spalding, "A novel finite difference formulation for diferential equations involving both first and second derivatives", *Int. J. Num. Meth. Eng.*, **4**, 551–9, 1972.

[43] K.E. Barrett, "The numerical solution of singular perturbation boundary value problem", *Q. J. Mech. Appl. Math.*, **27**, 57–68, 1974.

[44] O.C. Zienkiewicz, J.C. Heinrich, P.S. Huyakorn and A.R. Mitchel, "An upwind finite element scheme for two dimensional convective transport equations", *Int. J. Num. Meth. Eng.*, **11**, 131–44, 1977.

[45] J. Douglas and J. Wang, "An absolutely stabilized finite element method for the Stokes problem", *Math. Comput.*, **52**, 495-508, 1989.

[46] R. Codina, "On stabilized finite element method for non linear system of convection-diffusion-reaction equations", Publication CIMNE, PI-126, December 1997. To be published in *Comp. Meth. Appl. Mech. Engng.*

[47] T.J.R. Hughes and M. Mallet, “A new finite element formulations for computational fluid dynamics: IV. A discontinuity capturing operator for multidimensional advective-diffusive system, *Comput. Meth. Appl. Mech. Engng.*, **58**, 329–336, 1986.

[48] A.C. Galeao and E.G. Dutra do Carmo, “A consistent approximate upwind Petrov-Galerkin method for convection dominated problems”, *Comput. Meth. Appl. Mech. Engng.*, **68**, 83–95, 1988.

[49] R. Codina, “A discontinuity-capturing crosswind dissipation for the finite element solution of the convection-diffusion equation”, *Comput. Meth. Appl. Mech. Engng.*, **110**, 325–342, 1993.

[50] O.C. Zienkiewicz and J.Z. Zhu, “The supercorvergent patch recovery (SPR) and adaptive finite element refinement”, *Comp. Meth. Appl. Mech. Engng.*, **101**, 207–224, 1992.

[51] N.-E. Wiberg, F. Abdulwahab and X.D. Li, “Error estimation and adaptive procedures based on superconvergent patch recovery (SPR)”, *Archives of Computational Methods in Engineering*, Vol. **4** (3), 203– 242, (1997).

[52] P.D. Lax and B. Wendroff, ”Systems of conservative laws”, *Comm. Pure Appl. Math.*, **13**, 217–37, 1960.

[53] F. Shakib, “Finite Element Analysis of the Compressible Euler and Navier-Stokes Equations”, *Ph. Thesis, Division of Appl. Mechanics*, Stanford Univ., 1989.